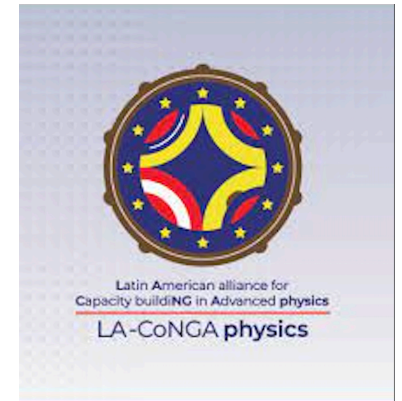




Proximity Effects and spintronics in low dimensional systems

Ernesto Medina

Departamento de Física, USFQ



Proximity Effects and spintronics in low dimensional systems

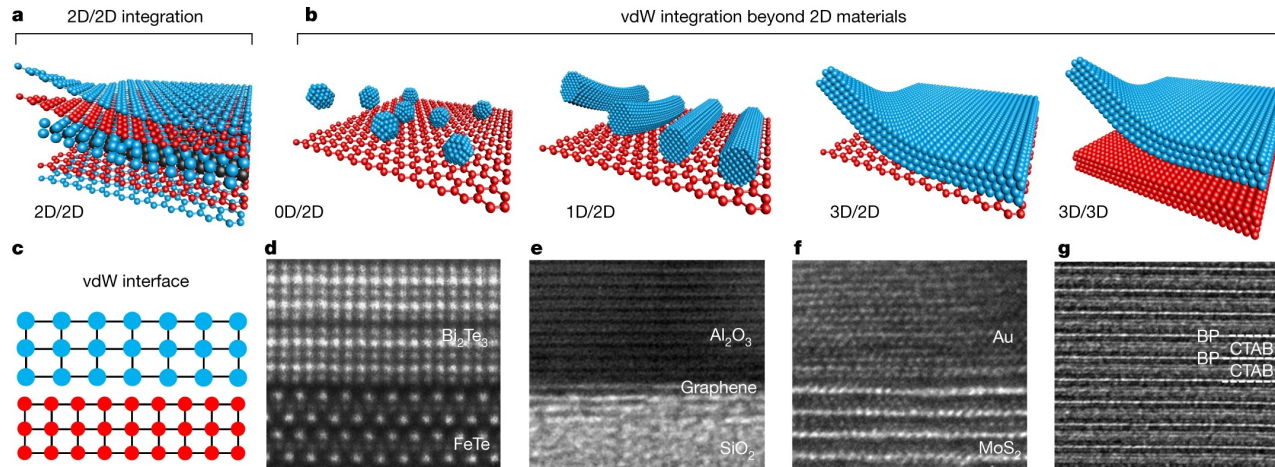
Ernesto Medina

Departamento de Física, USFQ

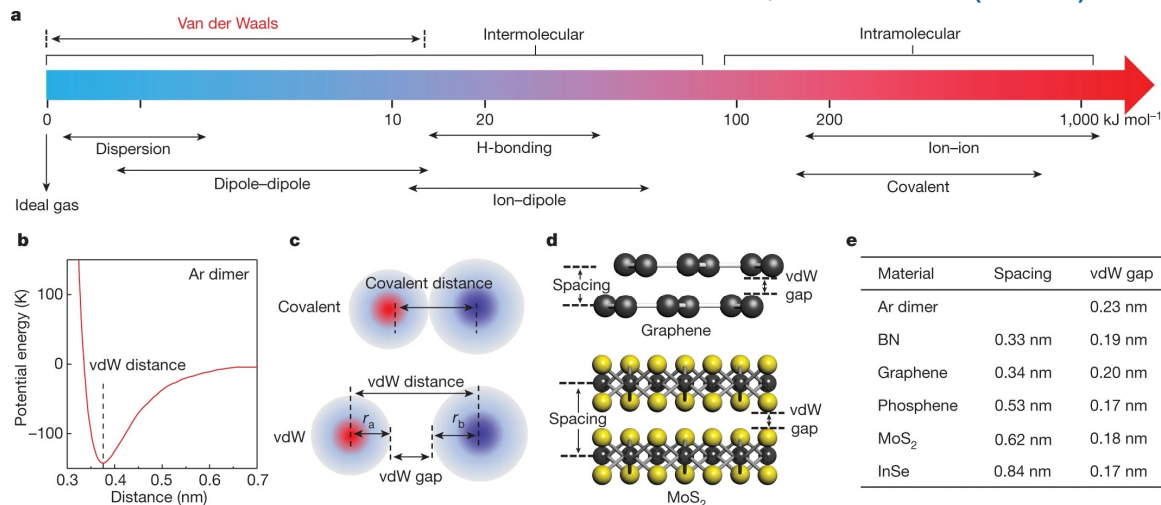
Summary

- Clarity of simplest models versus ab initio calculations, the case of Ni/Co and Au on graphene: Band folding/Matrix perturbation theory
 - Ferro and AntiFerro on graphene without degrading its properties
 - Strong spin-orbit coupling induced by Au
- Spin activity in the absence of exchange interactions and magnetic centers. The case of CISS
 - Chiral molecules as a spin polarizers
 - Hydrogen bonding generate Rashba interactions
 - Stretching molecules and Molecular spectroscopy/SO enhancement

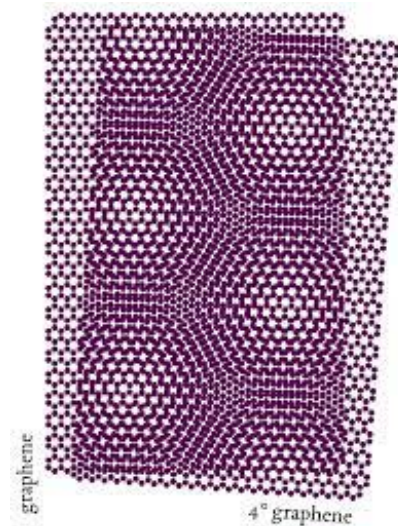
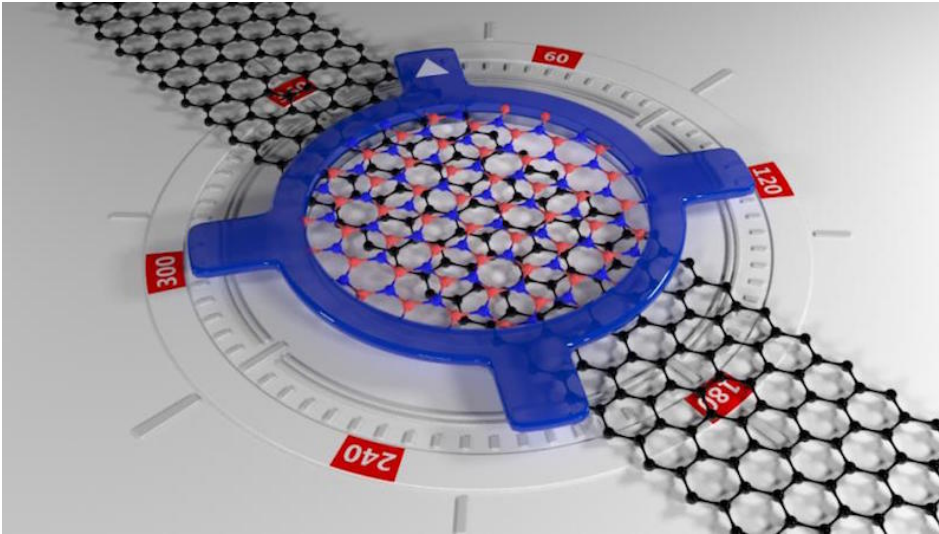
Van der Waals Materials/Proximity coupling



Liu, Huang, Duan, Nature volume, 567, 323–333 (2019)

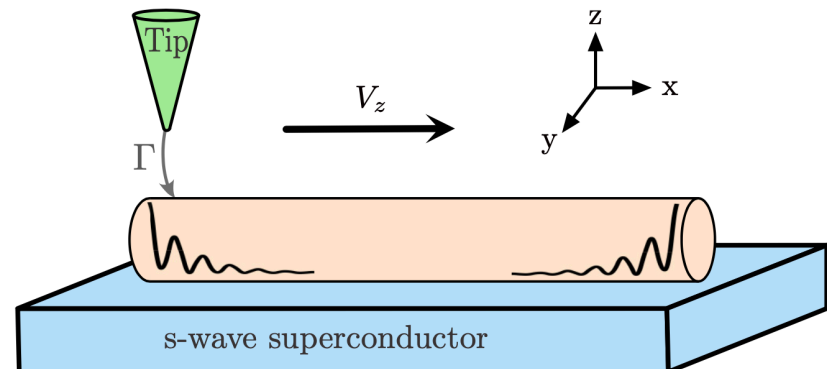


Twistronics/Majorana

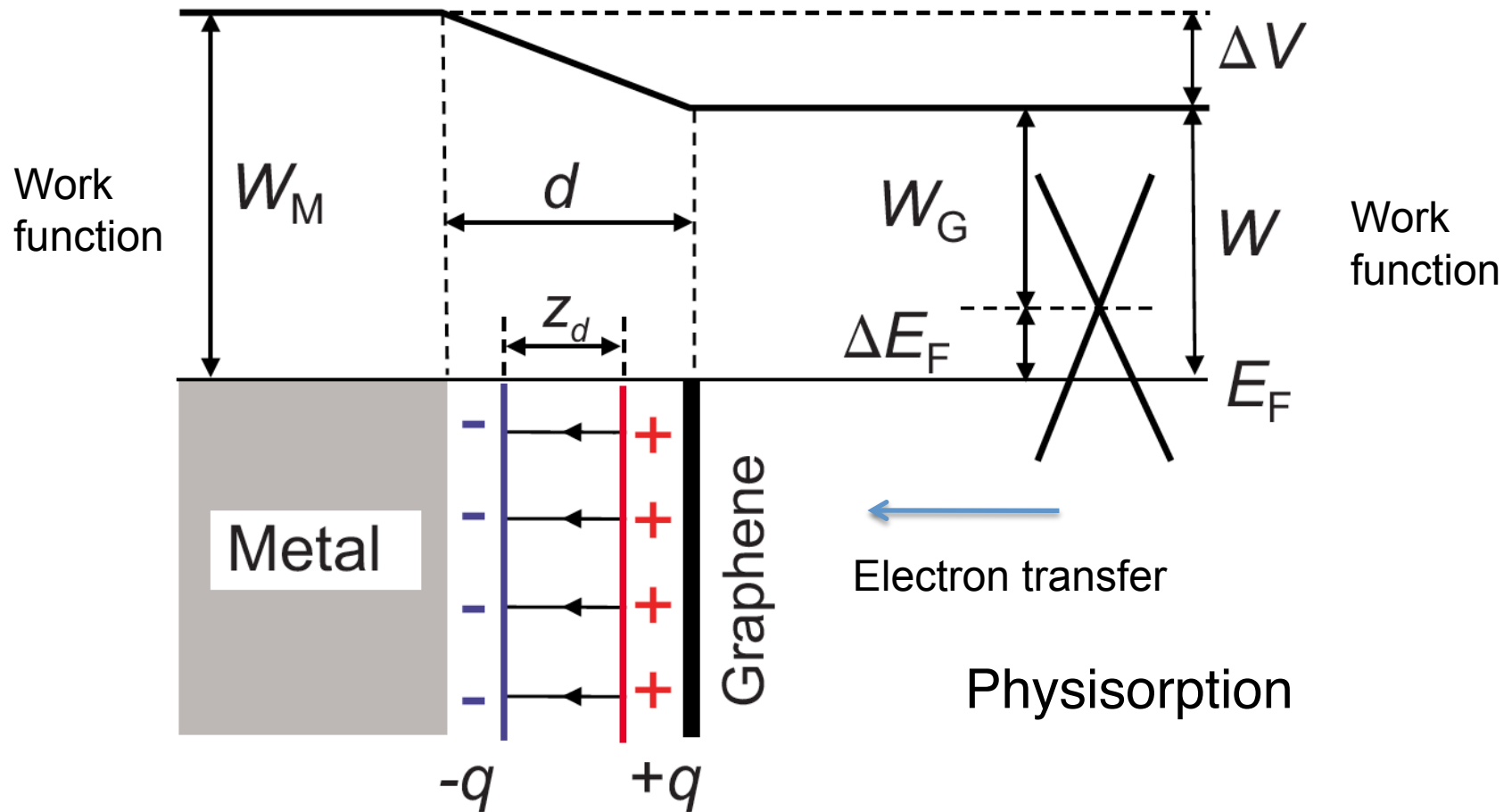


Magic angles at which the fermi velocity $\rightarrow 0$
then magnetism and superconductivity arise

Rashba (SO coupling) nanowire on
superconductor

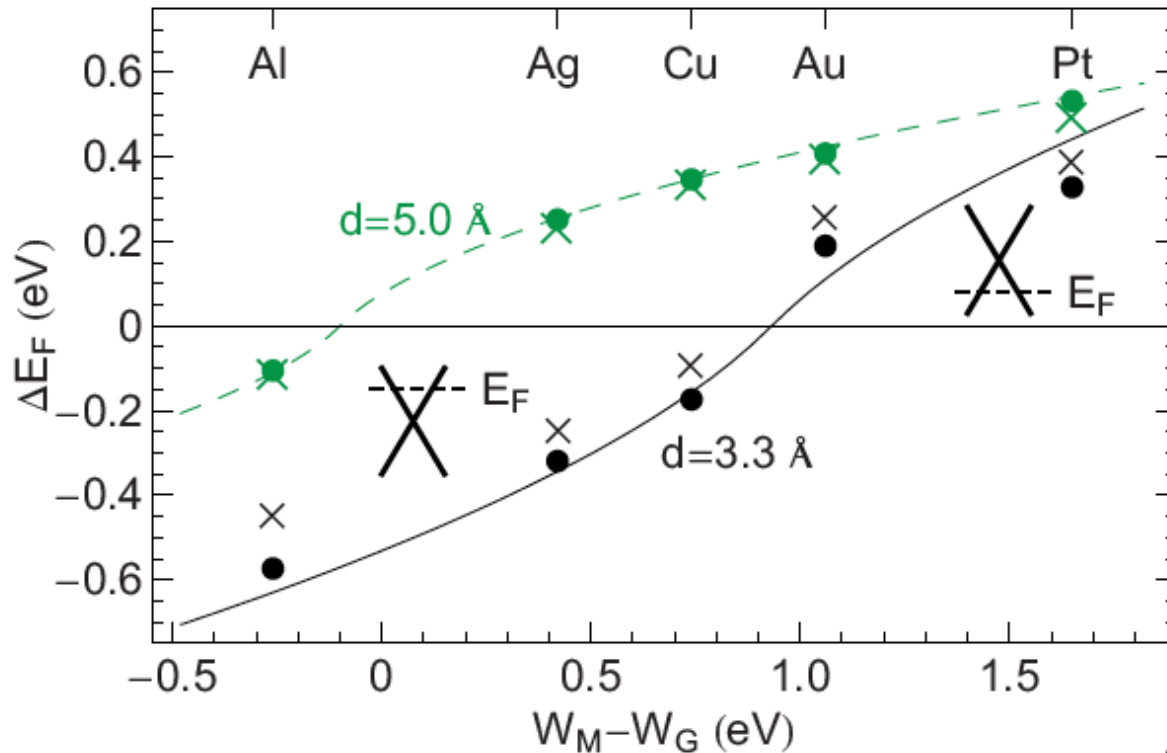


Proximity regimes: Substrate effects



Khomyakov et al (2009)

Changes in chemical potential



Δ work function Wave-f overlap

$$\Delta V(d) = \Delta_{\text{tr}}(d) + \Delta_c(d)$$

$W - W_G$ (eV)

Wave-function overlap

$$\Delta_c(d) = e^{-\gamma d} (a_0 + a_1 d + a_2 d^2)$$

$$\Delta E_F(d) = \pm \frac{\sqrt{1 + 2\alpha D_0(d - d_0)|W_M - W_G - \Delta_c(d)|} - 1}{\alpha D_0(d - d_0)}$$

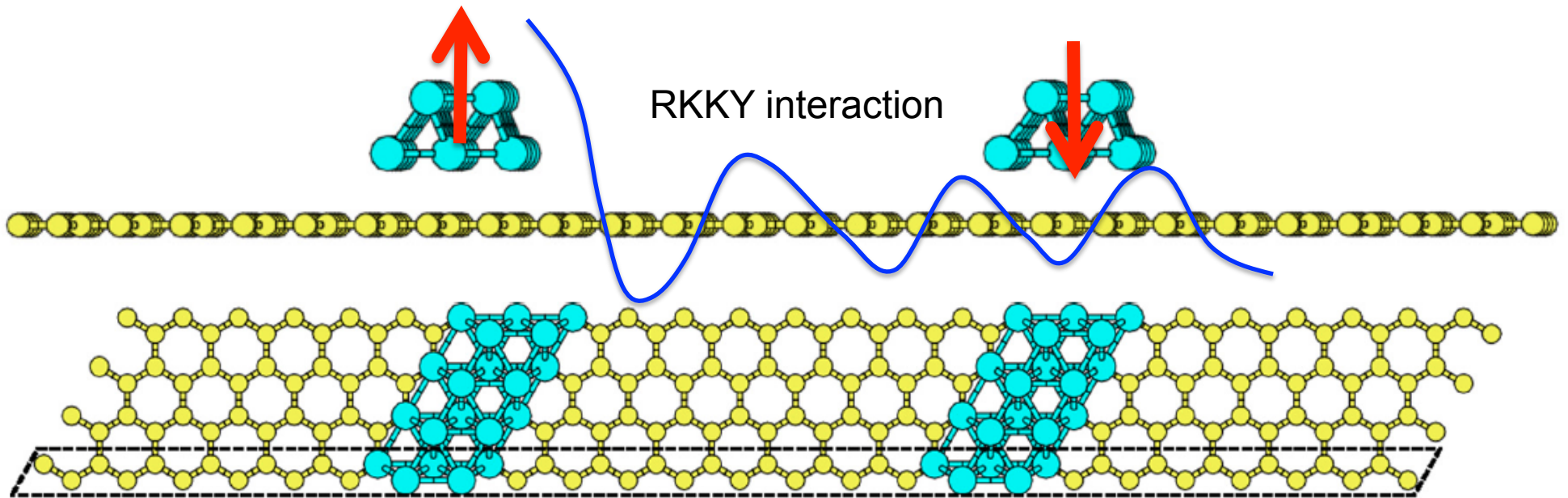
DOS

$$D(E) = D_0|E|$$

Why proximity effects?

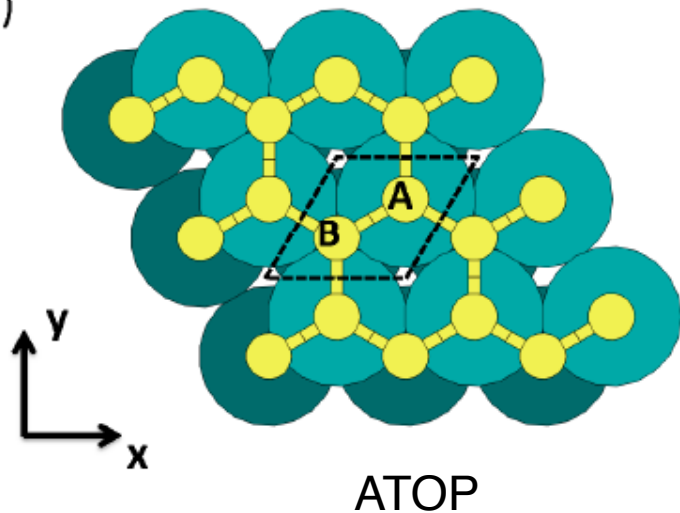
- Defects and impurities reduce desirable mobility properties
- Can dope n or p with metals gauging the distance without gating (graphene has no carriers without doping)
- Can induce spin-orbit interaction without substitutional heavy atoms
- Induce A-B asymmetries for semiconducting properties

Proximity effects: Co over graphene



(a)

Graphene



The sign of the interaction can be manipulated by a gate voltage

BUT! Coupling produces AF interactions!

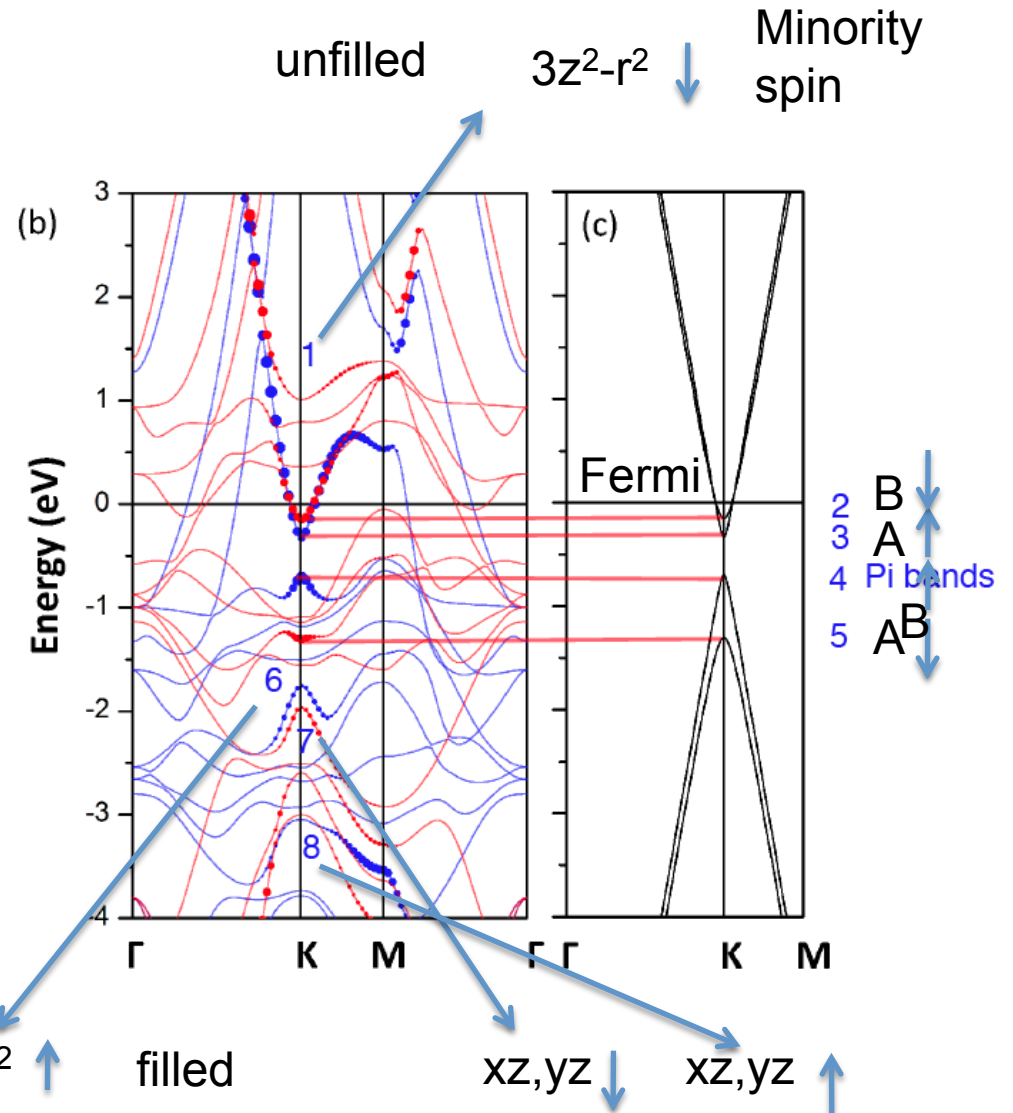
McDonald et al PRB 2013

Co-Graphene bands

ATOP configuration

TABLE I. Orbital character of the bands in Fig. 1(b) at the K point of the 2D Brillouin zone. Only those having strong carbon p_z characters are listed. A and B correspond to the two sublattices of graphene, as shown in Fig. 1(a).

Band No.	Energy (eV)	C p_z character	Co d character
1	1.006	A \downarrow : 0.069	$3z^2 - r^2\downarrow$: 0.671
2	-0.151	B \downarrow : 0.319	$xz, yz\downarrow$: 0.098 $x^2 - y^2, xy\downarrow$: 0.099
3	-0.328	A \uparrow : 0.297	$3z^2 - r^2\uparrow$: 0.368
4	-0.703	B \uparrow : 0.439	$xz, yz\uparrow$: 0.059 $x^2 - y^2, xy\uparrow$: 0.016
5	-1.307	A \downarrow : 0.341	$3z^2 - r^2\downarrow$: 0.019
6	-1.754	A \uparrow : 0.191	$3z^2 - r^2\uparrow$: 0.303
7	-1.965	B \downarrow : 0.185	$xz, yz\downarrow$: 0.19 $x^2 - y^2, xy\downarrow$: 0.054
8	-3.048	B \uparrow : 0.055	$xz, yz\uparrow$: 0.206 $x^2 - y^2, xy\uparrow$: 0.166



Mixed with A π orbital/ Majority spin

3z²-r² ↑ filled

xz, yz ↓

xz, yz ↑

Proximity effects: Co over graphene

Empirical model McDonald et al 2012

$$H = \mu + \hbar v_F k \cdot \sigma - h_{0z} \sigma_z - h_{z0} s_z - h_{zz} s_z \sigma_z$$

Electron
transfer

Graphene

Asymmetric
Lattice/
pseudo
spin

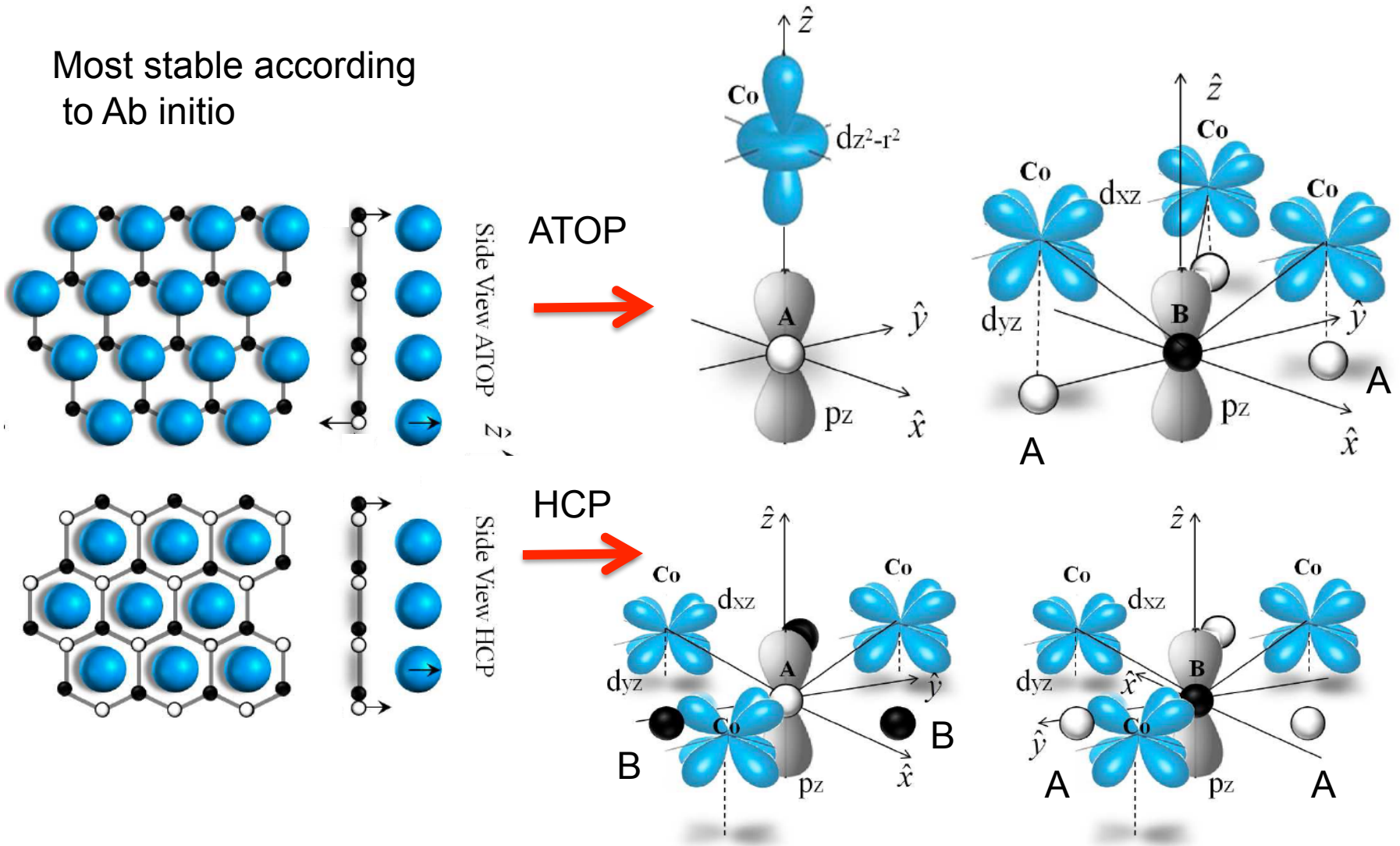
Asymmetric
spin

Asymmetric
Spin/pseudospin

We can derive it from tight binding and determine the coefficients
Design appropriately each term

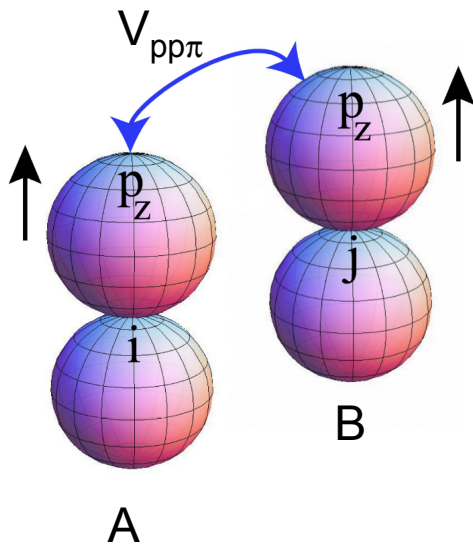
Lattice registries

Most stable according to Ab initio

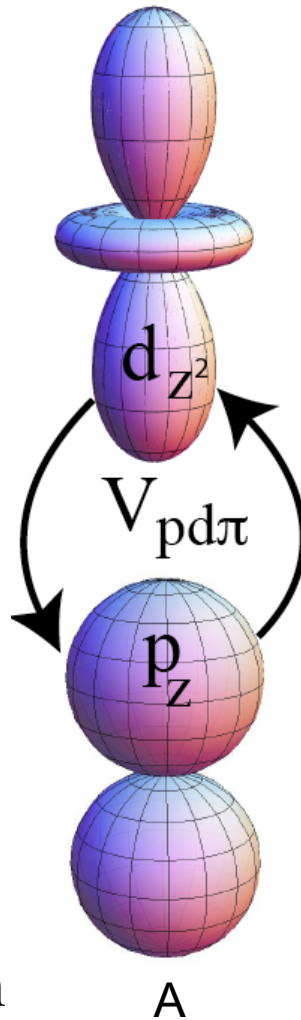


Atop configuration

Process on graphene

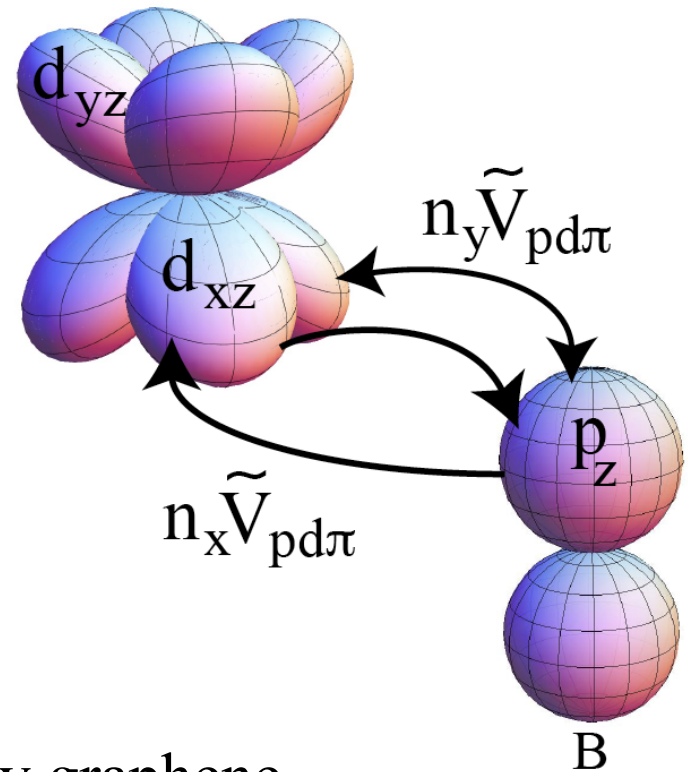


Also magnetization
Dependent correction



A

Hopping to Co/Ni



B

Only graphene
site energies corrected

Co over graphene couplings

H_γ
 T

	A,Pz	B,Pz	d_z^2	d_{xz}	d_{yz}
A,Pz	ϵ_p	$V_{pp\tau}$	V_{pdz^2}	0	0
B,Pz	$V_{pp\tau}$	ϵ_p	0	$\hat{n}_x \tilde{V}_{pd\tau}$	$\hat{n}_y \tilde{V}_{pd\tau}$
d_z^2	$-V_{pdz^2}$	0	$\epsilon_{dz^2} + \delta_1 s_z$	0	0
d_{xz}	0	$-\hat{n}_x \tilde{V}_{pd\tau}$	0	$\epsilon_{dxz} + \delta_2 s_z$	0
d_{yz}	0	$-\hat{n}_y \tilde{V}_{pd\tau}$	0	0	$\epsilon_{dyz} + \delta_2 s_z$

Want an effective $\mathcal{H}_{2 \times 2}$

Can also apply real space Feynman method

H_χ

Matrix perturbation theory

Instead of Feynman paths we use Foldy-Wouthuysen band folding approach

$$\begin{pmatrix} H_\gamma & T \\ T^\dagger & H_\chi \end{pmatrix} \begin{pmatrix} \gamma \\ \chi \end{pmatrix} = E \begin{pmatrix} \gamma \\ \chi \end{pmatrix}$$

$$T^\dagger \gamma + H_\chi \chi = E \chi$$

$$H_\gamma \gamma + T \chi = E \gamma$$

$$T^\dagger \gamma = (E - H_\chi) \chi$$

$$\left(H_\gamma + T (E - H_\chi)^{-1} T^\dagger \right) \gamma = E \gamma$$

$$(E - H_\chi)^{-1} T^\dagger \gamma = \chi$$

Eigenvalues of
 $H_\chi > E$

$$\frac{1}{E - H_\chi} = - \frac{1}{H_\chi \left(1 - (H_\chi)^{-1} E \right)} = - \frac{1}{H_\chi} \left(1 + \frac{E}{H_\chi} + \dots \right)$$

Matrix perturbation theory

$$\left(H_\gamma - T \frac{1}{H_\chi} \left(1 + \frac{E}{H_\chi} + \dots \right) T^\dagger \right) \gamma = E\gamma$$

$$\left(H_\gamma - T \frac{1}{H_\chi} T^\dagger \right) \gamma = E\gamma + \left(T \frac{1}{H_\chi} \frac{E}{H_\chi} T^\dagger \right) \gamma = E \underbrace{\left(1 + T (H_\chi)^{-2} T^\dagger \right)}_S \gamma = ES\gamma$$

Define

$$\Phi = S^{1/2} \gamma \quad S^{-1/2} \Phi = \gamma$$

$$S^{-1/2} \left(H_\gamma - T \frac{1}{H_\chi} T^\dagger \right) S^{-1/2} \Phi = E\Phi$$

Matrix perturbation theory

$$\Phi^\dagger \Phi = \gamma^\dagger S^{1/2} S^{1/2} \gamma = \gamma^\dagger \left(1 + T (H_\chi)^{-2} T^\dagger \right) \gamma \approx \gamma^\dagger \gamma + \chi^\dagger \chi$$

Norm must be
Consistent in
perturbation

$$S^{-1/2} \left(H_\gamma - T \frac{1}{H_\chi} T^\dagger \right) S^{-1/2} \Phi = E \Phi$$

$$\mathcal{H}_{\text{eff}}$$

With dimension of H_γ

As γ is the subspace of p_z these orbitals are dressed by the couplings.

ATOP configuration

$$H_{ATOP} = - \sum_{\langle ij \rangle} \gamma_0 a_i^\dagger b_j - \frac{(\epsilon_p - \epsilon_d) + \delta_1 s_z}{(\epsilon_p - \epsilon_d)^2 - \delta_1^2} v_{pdz}^2 \sum_i a_i^\dagger a_i$$

$$- 3 \frac{(\epsilon_p - \epsilon_d) + \delta_2 s_z}{(\epsilon_p - \epsilon_d)^2 - \delta_2^2} \tilde{v}_{pd\pi}^2 \sum_j b_j^\dagger b_j$$

Magnetic order in Co

coordination of first neighbours

Perturbed Site energies

Full Brillouin zone

ATOP in vicinity of K points

$$H_{\text{ATOP}}(\mathbf{k}) = \begin{pmatrix} \mu - h_{0z} - \frac{h_{z0}}{2} - \frac{h_{zz}}{2} & v(\xi p_x - ip_y) & 0 & 0 \\ v(\xi p_x + ip_y) & \mu - h_{0z} + \frac{h_{z0}}{2} + \frac{h_{zz}}{2} & 0 & 0 \\ 0 & 0 & \mu + h_{0z} - \frac{h_{z0}}{2} + \frac{h_{zz}}{2} & v(\xi p_x - ip_y) \\ 0 & 0 & v(\xi p_x + ip_y) & \mu + h_{0z} + \frac{h_{z0}}{2} - \frac{h_{zz}}{2} \end{pmatrix}$$

$$H_{\text{ATOP}}(k=0) = \mu \hat{\uparrow}_\sigma \hat{\uparrow}_s - h_{0z} \sigma_z \hat{\uparrow}_s - \frac{h_{z0}}{2} \hat{\uparrow}_\sigma s_z - \frac{h_{zz}}{2} \sigma_z s_z$$

The McDonald Hamiltonian

$$\begin{aligned} -\frac{V_{pdz}^2 (\varepsilon_p - \varepsilon_d)}{(\varepsilon_p - \varepsilon_d)^2 - \delta_1^2} &= \mu - h_{0z}, & \frac{\delta_1 V_{pdz}^2}{(\varepsilon_p - \varepsilon_d)^2 - \delta_1^2} &= \frac{(h_{z0} + h_{zz})}{2} \\ -3 \frac{\tilde{V}_{pd\pi}^2 (\varepsilon_p - \varepsilon_d)}{(\varepsilon_p - \varepsilon_d)^2 - \delta_2^2} &= \mu + h_{0z}, & 3 \frac{\delta_2 \tilde{V}_{pd\pi}^2}{(\varepsilon_p - \varepsilon_d)^2 - \delta_2^2} &= \frac{(h_{z0} - h_{zz})}{2} \end{aligned}$$

ATOP in vicinity of K points

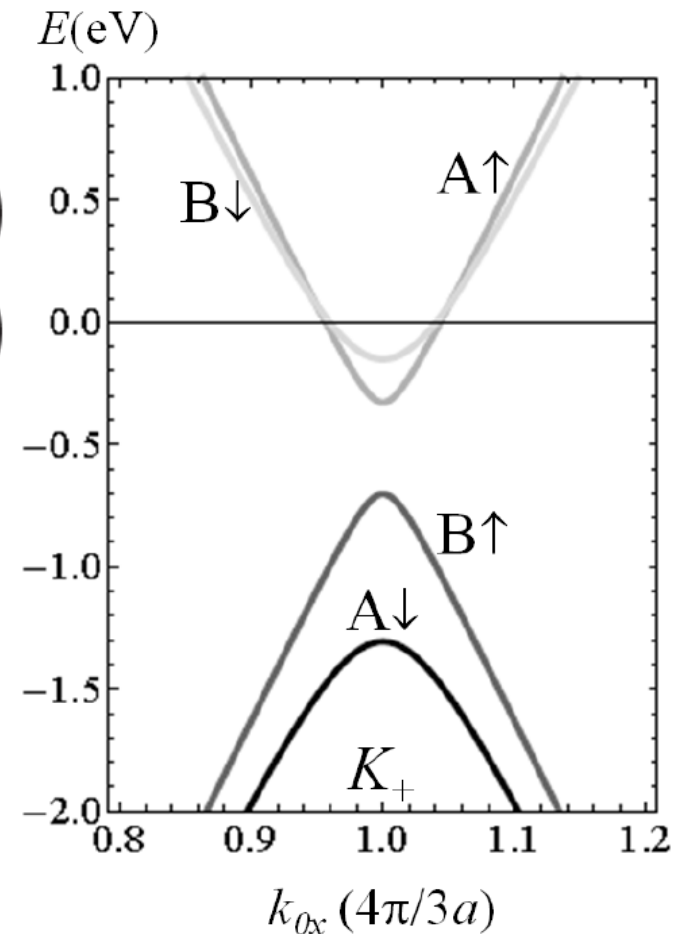
$$\epsilon_v(\mathbf{k}) = \frac{1}{2} \left(2\mu - s_z h_{z0} - \sqrt{(2h_{0z} + s_z h_{zz})^2 + 4v^2 \hbar^2 |\mathbf{k}|^2} \right)$$
$$\epsilon_c(\mathbf{k}) = \frac{1}{2} \left(2\mu - s_z h_{z0} + \sqrt{(2h_{0z} + s_z h_{zz})^2 + 4v^2 \hbar^2 |\mathbf{k}|^2} \right)$$

A sublattice AF wrt Co

B sublattice F wrt Co

Result: AF with a slightly higher
Spin component opposite to Co

Depending on overlaps and coordination



HCP real space Hamiltonian

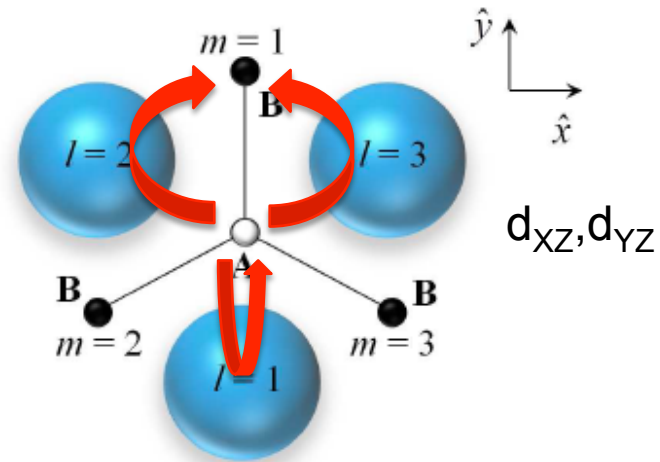
H_γ
 T

	A,Pz	B,Pz	d_z^2	d_{xz}	d_{yz}
A,Pz	ϵ_p	$V_{pp\tau}$	0	$\hat{n}_x \tilde{V}_{pd\tau}$	$\hat{n}_y \tilde{V}_{pd\tau}$
B,Pz	$V_{pp\tau}$	ϵ_p	0	$\hat{n}_x \tilde{V}_{pd\tau}$	$\hat{n}_y \tilde{V}_{pd\tau}$
d_z^2	0	0	$\epsilon_{dz^2} + \delta_1 s_z$	0	0
d_{xz}	$-\hat{n}_x \tilde{V}_{pd\tau}$	$-\hat{n}_x \tilde{V}_{pd\tau}$	0	$\epsilon_{dxz} + \delta_2 s_z$	0
d_{yz}	$-\hat{n}_y \tilde{V}_{pd\tau}$	$-\hat{n}_y \tilde{V}_{pd\tau}$	0	0	$\epsilon_{dyz} + \delta_2 s_z$

Want an effective $\mathcal{H}_{2 \times 2}$

H_χ

HCP bands



$$H_{\text{HCP}}(\mathbf{k}) = \begin{pmatrix} -3 \frac{\varepsilon + \delta_2}{\varepsilon^2 - \delta_2^2} \tilde{V}_{pd\pi}^2 & 0 & -\frac{v}{\gamma_0} (-\gamma_0 + \frac{\varepsilon + \delta_2}{\varepsilon^2 - \delta_2^2} \tilde{V}_{pd\pi}^2) p^* & 0 \\ 0 & -3 \frac{\varepsilon - \delta_2}{\varepsilon^2 - \delta_2^2} \tilde{V}_{pd\pi}^2 & 0 & -\frac{v}{\gamma_0} (-\gamma_0 + \frac{\varepsilon - \delta_2}{\varepsilon^2 - \delta_2^2} \tilde{V}_{pd\pi}^2) p^* \\ -\frac{v}{\gamma_0} (-\gamma_0 + \frac{\varepsilon + \delta_2}{\varepsilon^2 - \delta_2^2} \tilde{V}_{pd\pi}^2) p & 0 & -3 \frac{\varepsilon + \delta_2}{\varepsilon^2 - \delta_2^2} \tilde{V}_{pd\pi}^2 & 0 \\ 0 & -\frac{v}{\gamma_0} (-\gamma_0 + \frac{\varepsilon - \delta_2}{\varepsilon^2 - \delta_2^2} \tilde{V}_{pd\pi}^2) p & 0 & -3 \frac{\varepsilon - \delta_2}{\varepsilon^2 - \delta_2^2} \tilde{V}_{pd\pi}^2 \end{pmatrix}$$

$$\epsilon_v(\mathbf{k}) = -\mu' + s_z h'_{z0} + \frac{v\hbar}{\gamma_0} (-\gamma_0 - h'_{0x} + s_z h'_{zx}) |\mathbf{k}|$$

$$\epsilon_c(\mathbf{k}) = -\mu' + s_z h'_{z0} - \frac{v\hbar}{\gamma_0} (-\gamma_0 - h'_{0x} + s_z h'_{zx}) |\mathbf{k}|$$

HCP Bands

$$H_{\text{HCP}}(\mathbf{k}) = -\mu' \begin{pmatrix} A\uparrow+B\uparrow & A\downarrow+B\downarrow & A\uparrow-B\uparrow & A\downarrow-B\downarrow \\ 1 & 0 & 0 & 0 \\ 0 & 1 & 0 & 0 \\ 0 & 0 & 1 & 0 \\ 0 & 0 & 0 & 1 \end{pmatrix} + \frac{v\hbar}{\gamma_0} |\mathbf{k}| (h'_{0x} + \gamma_0) \begin{pmatrix} A\uparrow+B\uparrow & A\downarrow+B\downarrow & A\uparrow-B\uparrow & A\downarrow-B\downarrow \\ 1 & 0 & 0 & 0 \\ 0 & 1 & 0 & 0 \\ 0 & 0 & -1 & 0 \\ 0 & 0 & 0 & -1 \end{pmatrix}$$

$$- h'_{z0} \begin{pmatrix} A\uparrow+B\uparrow & A\downarrow+B\downarrow & A\uparrow-B\uparrow & A\downarrow-B\downarrow \\ 1 & 0 & 0 & 0 \\ 0 & -1 & 0 & 0 \\ 0 & 0 & 1 & 0 \\ 0 & 0 & 0 & -1 \end{pmatrix} + \frac{v\hbar}{\gamma_0} |\mathbf{k}| h'_{zx} \begin{pmatrix} A\uparrow+B\uparrow & A\downarrow+B\downarrow & A\uparrow-B\uparrow & A\downarrow-B\downarrow \\ 1 & 0 & 0 & 0 \\ 0 & -1 & 0 & 0 \\ 0 & 0 & -1 & 0 \\ 0 & 0 & 0 & 1 \end{pmatrix}$$

$$H_{\text{ATOP}}(k=0) = -\mu' \uparrow_{\sigma} \uparrow_s - \frac{v\hbar}{\gamma_0} |\mathbf{k}| (h'_{0x} + \gamma_0) \sigma_z \uparrow_s ; -h'_{z0} \uparrow_{\sigma} s_z$$

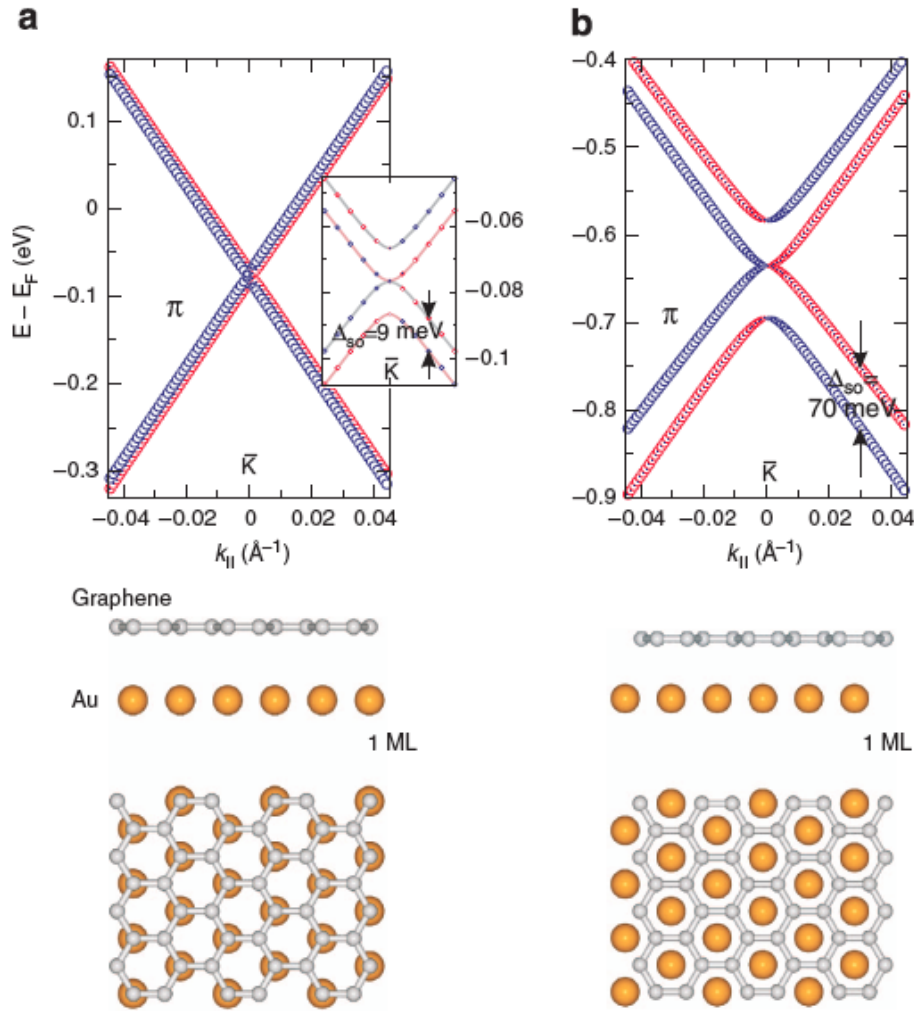
$$- \frac{v\hbar}{\gamma_0} |\mathbf{k}| h'_{zx} \sigma_z s_z$$

$$\langle S_z \rangle = \langle A\uparrow - B\uparrow | 1_{\sigma} S_z | A\uparrow - B\uparrow \rangle$$

$$= \frac{1}{2} (1 \ 0 \ -1 \ 0) \begin{pmatrix} 1 & 0 & 0 & 0 \\ 0 & -1 & 0 & 0 \\ 0 & 0 & 1 & 0 \\ 0 & 0 & 0 & -1 \end{pmatrix} \begin{pmatrix} 1 \\ 0 \\ -1 \\ 0 \end{pmatrix} = 1$$

Magnetization of states

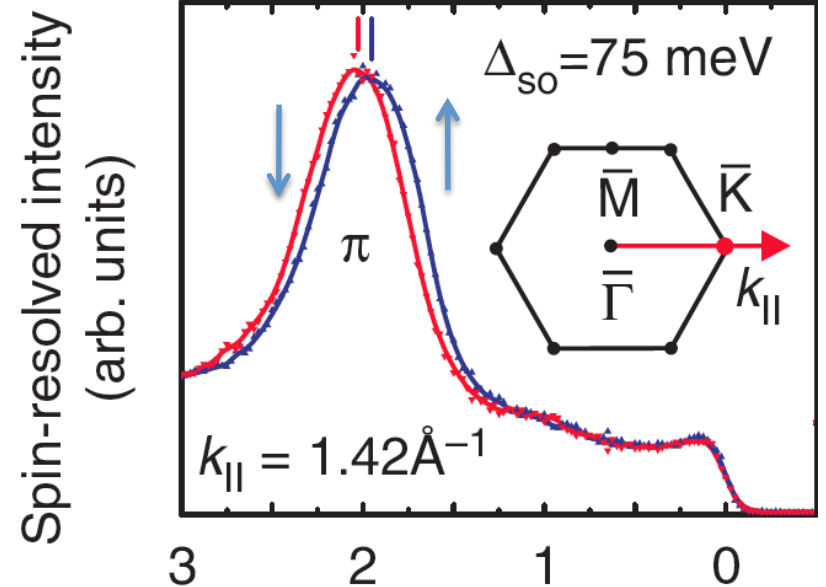
Enhancing SO on graphene



Heavy atom proximity effect

Marchenko et al 2012
Exp+DFT **Nature Comm.**

Spin resolved ARPES



spin-resolved photoemission

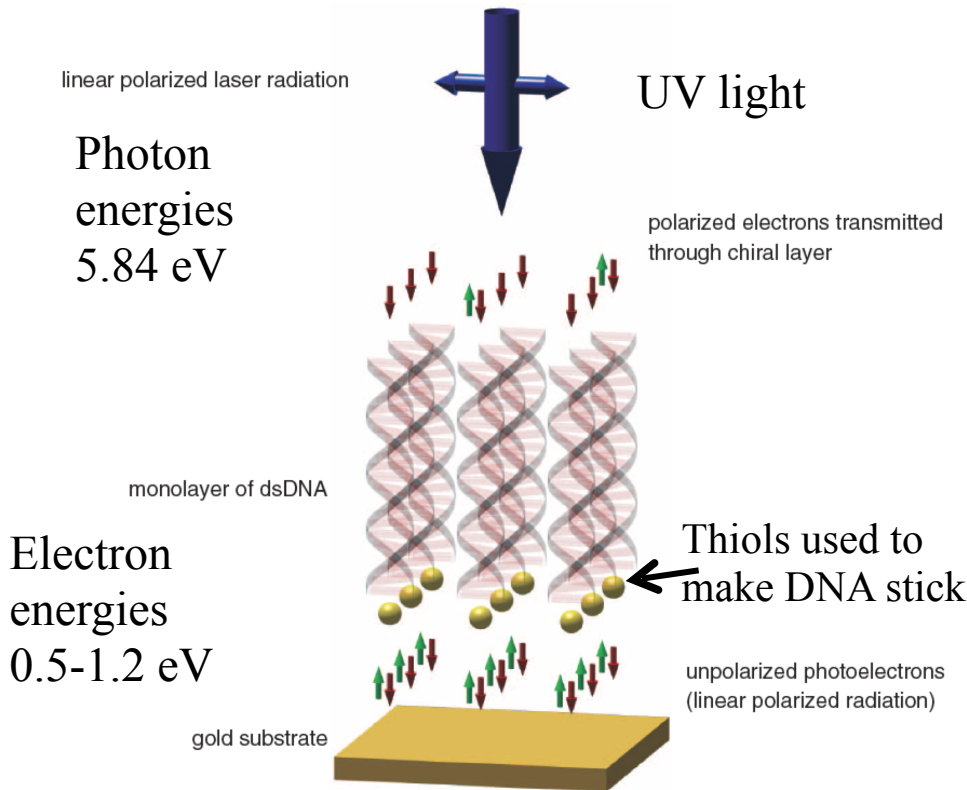
A. Lopez et al PRB (2019)

Experiments: Polarizing photoelectrons

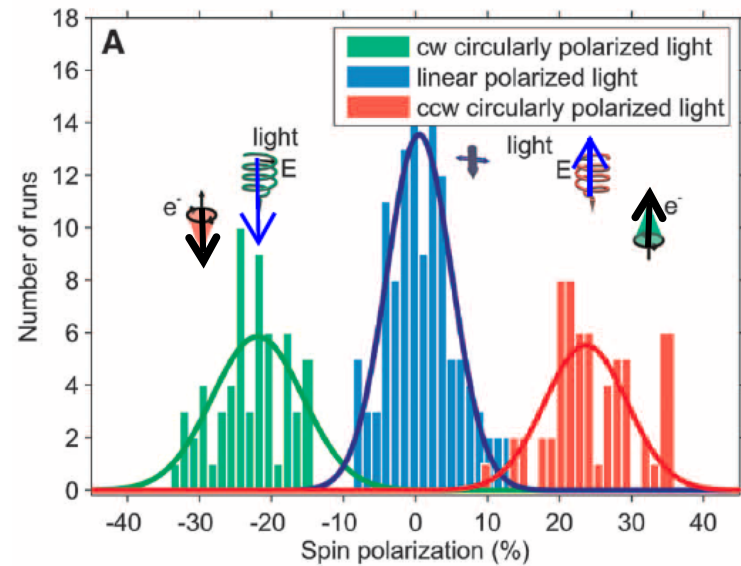
Spin Selectivity in Electron Transmission Through Self-Assembled Monolayers of Double-Stranded DNA

18 FEBRUARY 2011 VOL 331 SCIENCE

B. Göhler,¹ V. Hamelbeck,¹ T. Z. Markus,² M. Kettner,¹ G. F. Hanne,¹ Z. Vager,³
R. Naaman,^{2*} H. Zacharias¹

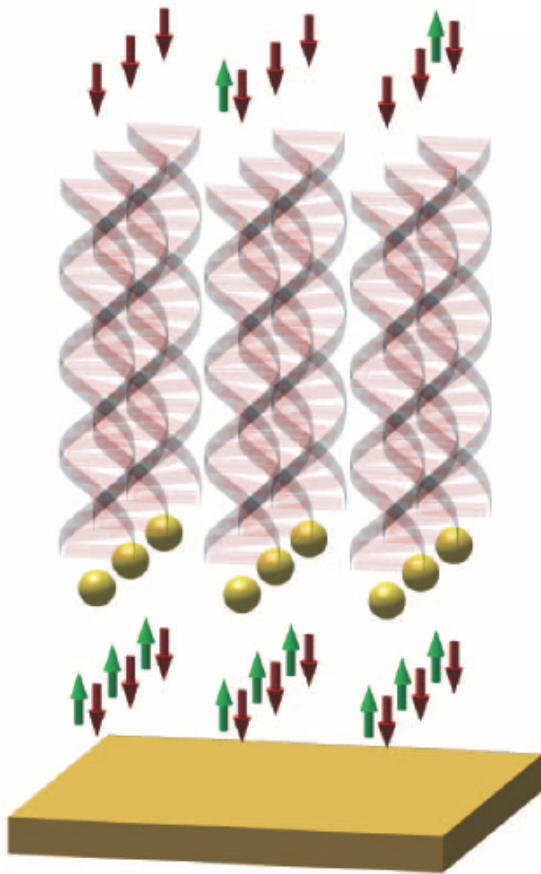


Bare surface



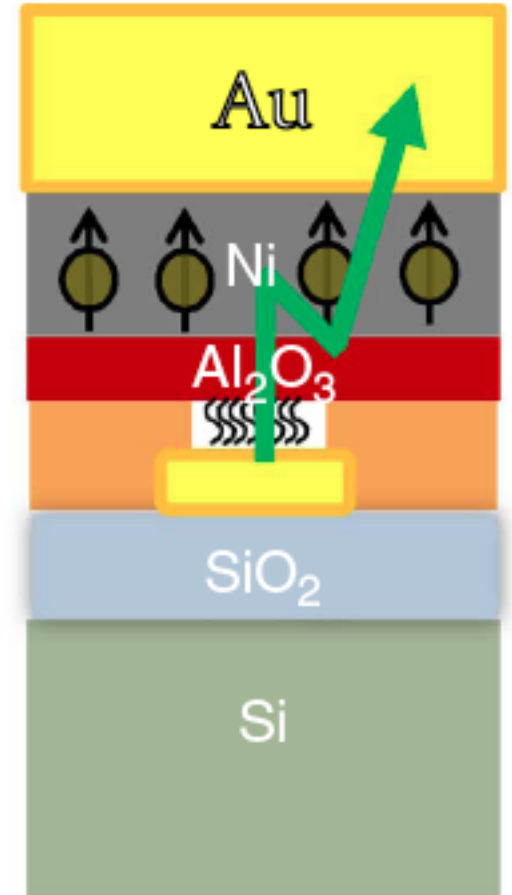
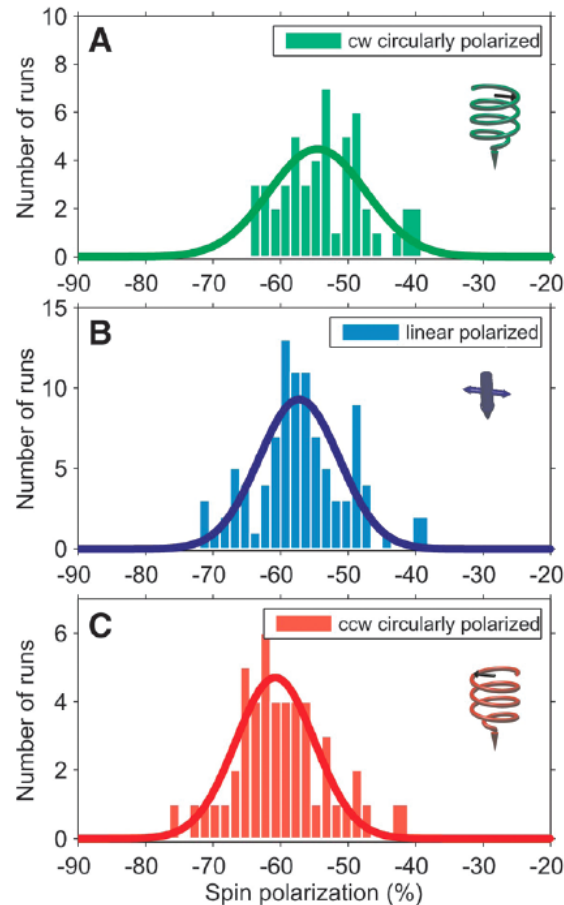
Electron polarization with organic molecules

Naaman Nanolett. 2011



Chirality → electron polarization

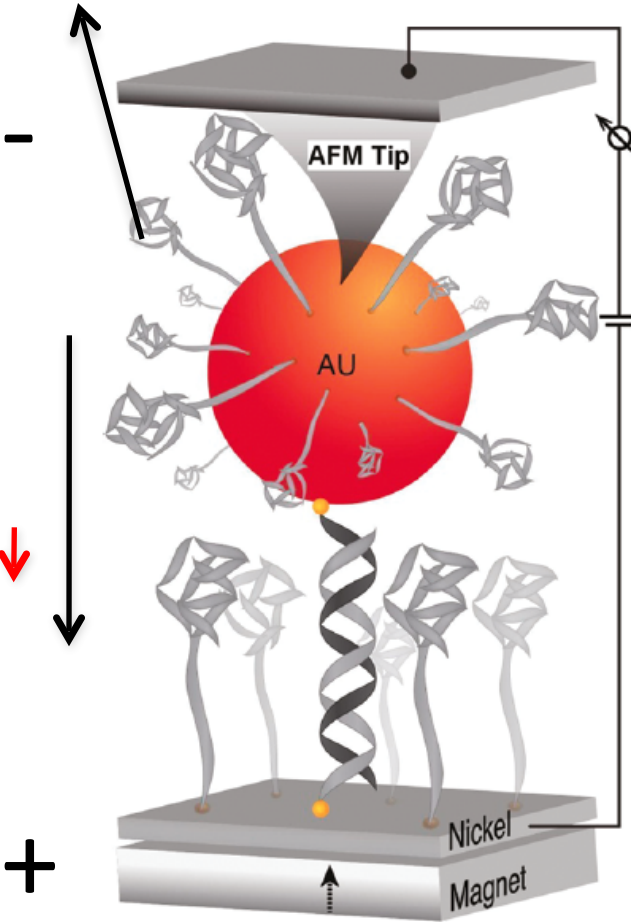
Nature 2013



Devices

Tunneling electron polarization

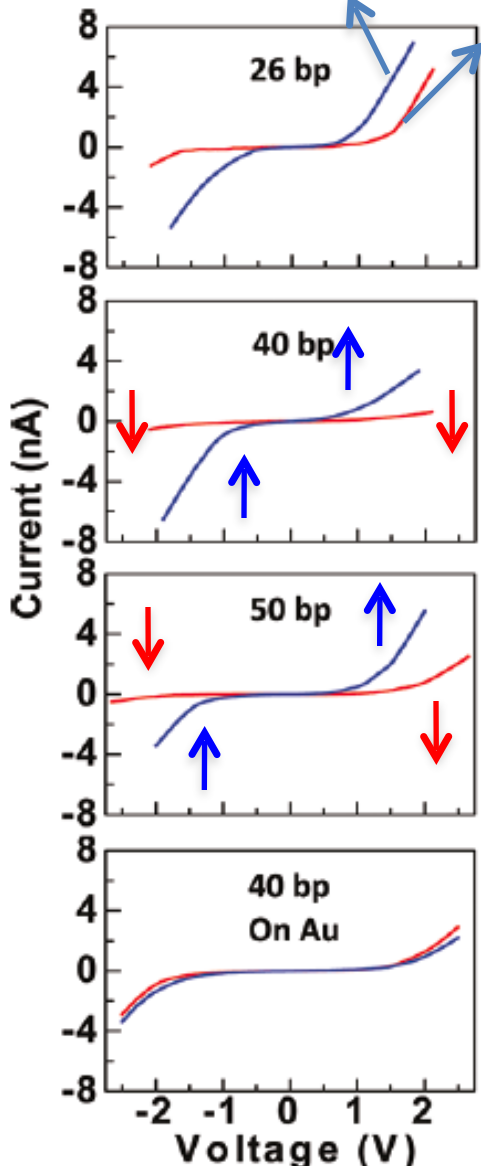
DNA separators



Single ds molecules

UP spin Ni

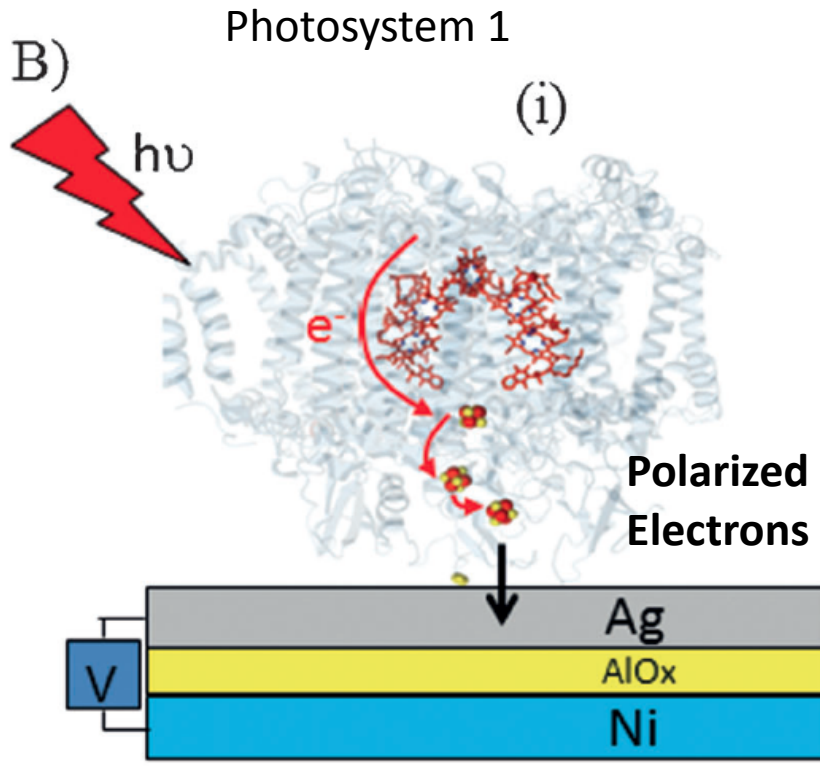
DOWN spin Ni



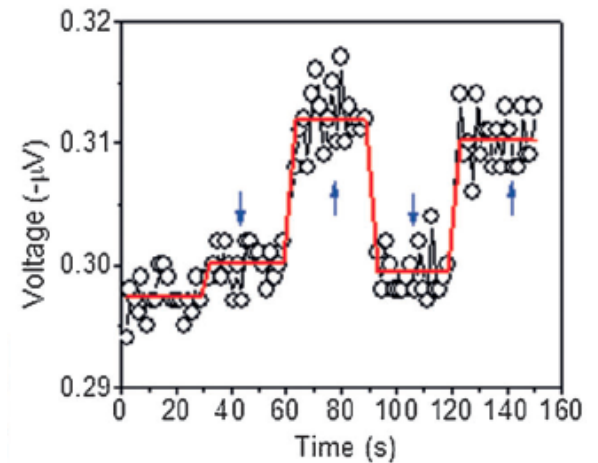
Xie et al Nanoletters 2011.

Barrier for transmission asymmetry between one spin orientation and the other

Photosystem 1



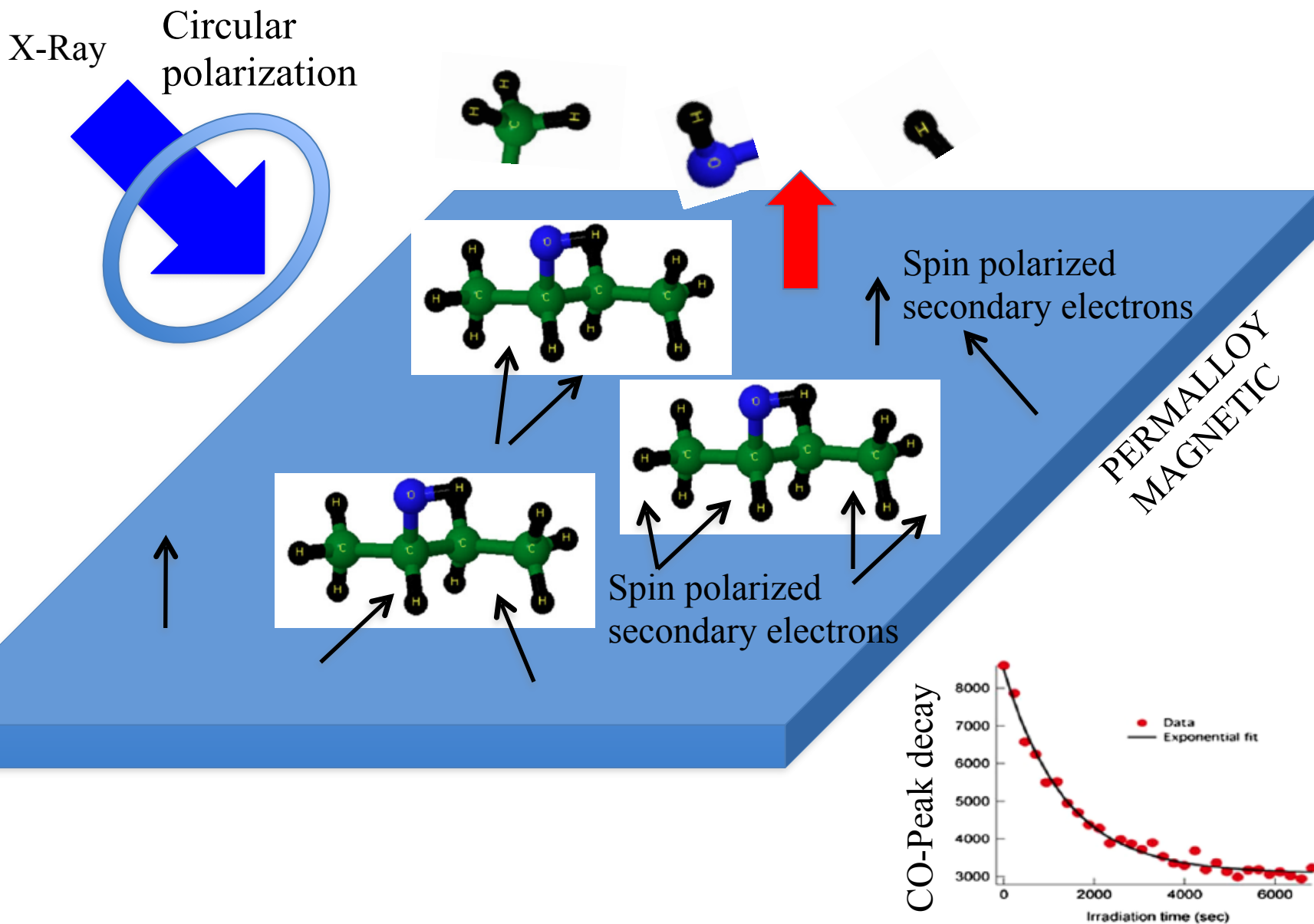
-Spin aligned parallel to momentum!
-Spin effect optimal at room temp,
degrades when you lower temp.



Ni orientation used to probe

Voltage between Ag and Ni tells spin accumulation orientation

Chiral reactions



Experiments: Chiral reactions spin sensitive

PRL 101, 178301 (2008)

PHYSICAL REVIEW LETTERS

week ending
24 OCTOBER 2008

Adsorbed
Butanol on
Permalloy

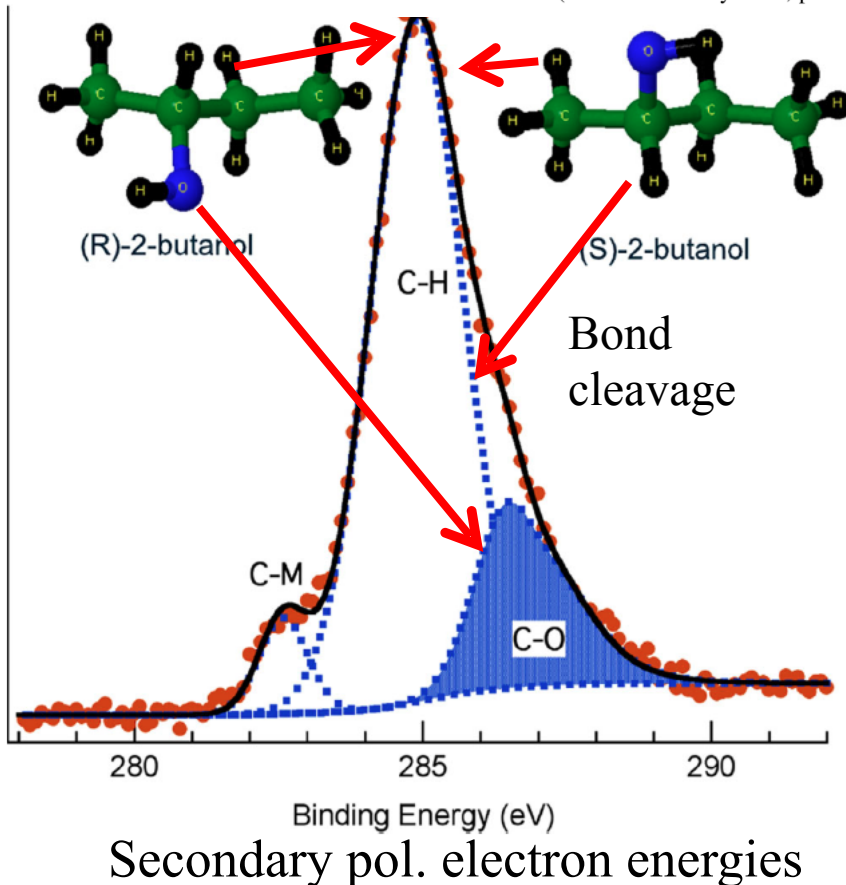
Chiral-Selective Chemistry Induced by Spin-Polarized Secondary Electrons from a Magnetic Substrate

R. A. Rosenberg,¹ M. Abu Haija,¹ and P.J. Ryan²

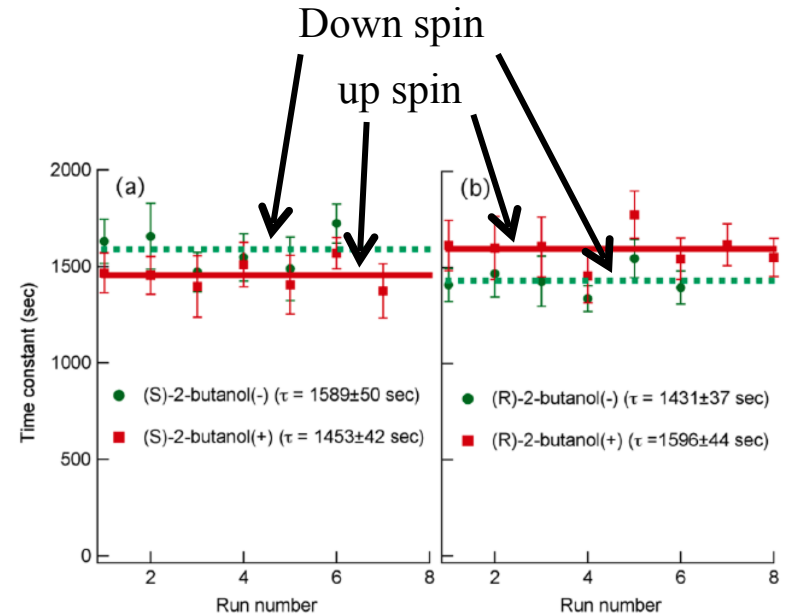
¹Advanced Photon Source, Argonne National Laboratory, Argonne, Illinois 60439, USA

²MUCAT, Ames Laboratory, Ames, Iowa 50011, USA

(Received 20 May 2008; published 21 October 2008)



Ease of cleavage
depends on
electron spin

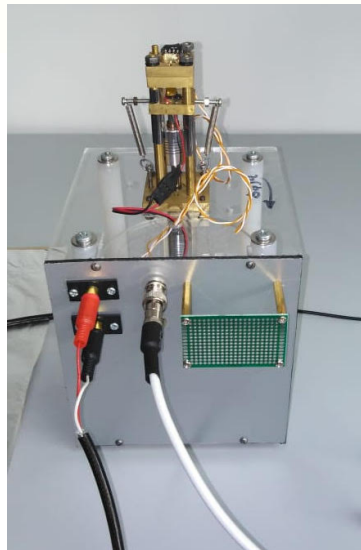
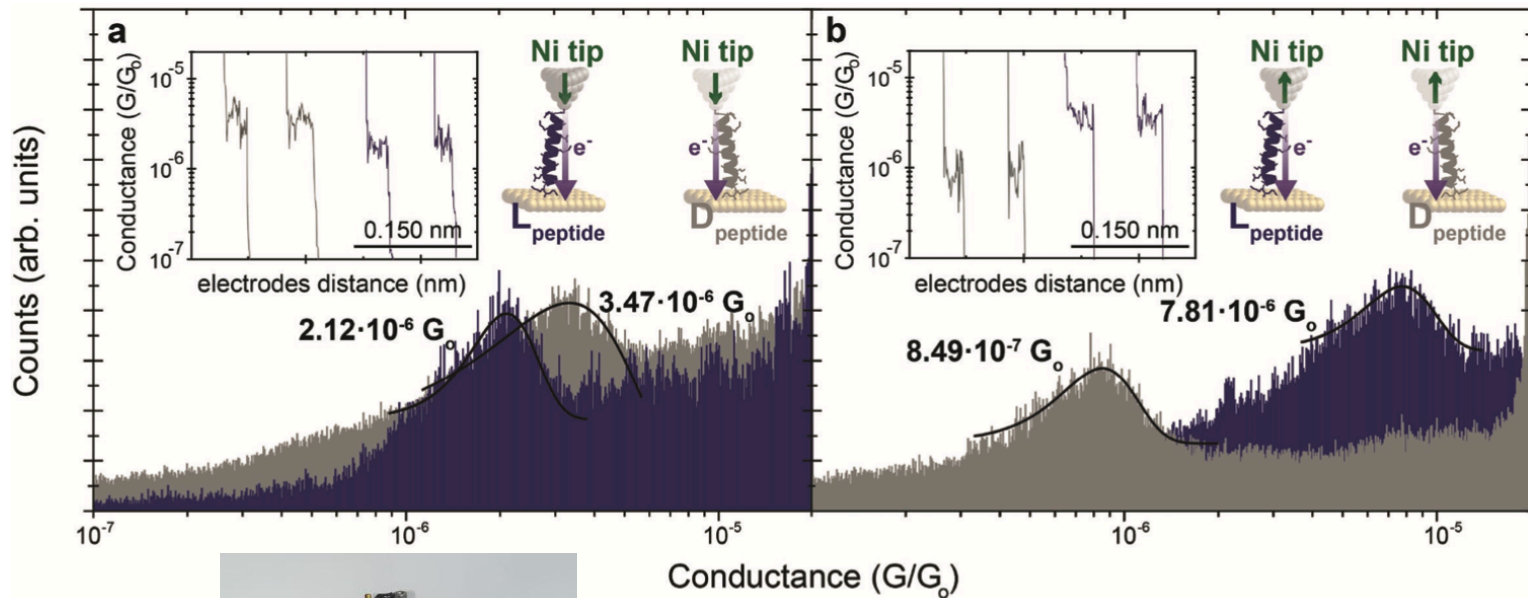


Spin torques involved?

→ SO interaction (No theory here)

Conductance Histograms

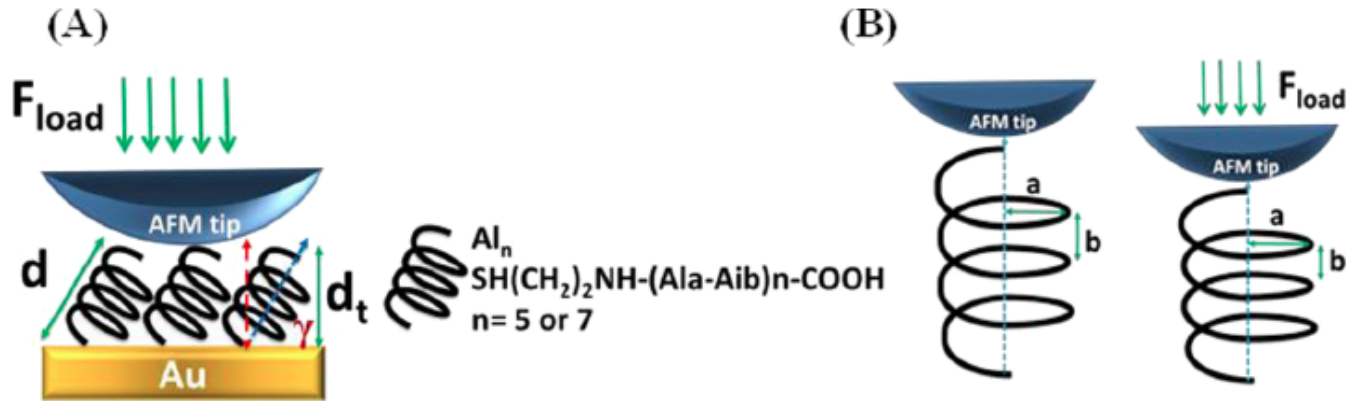
Aragones et al Small 2016



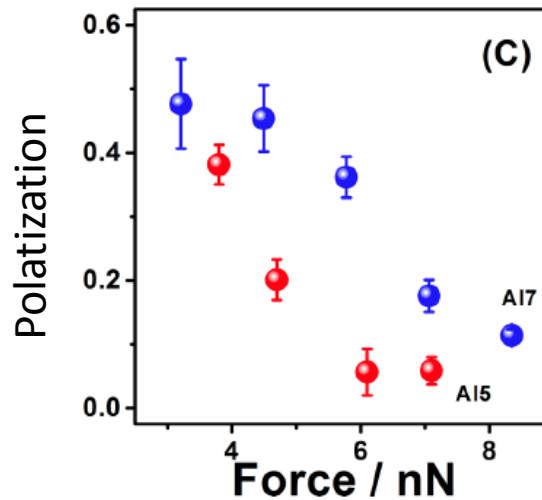
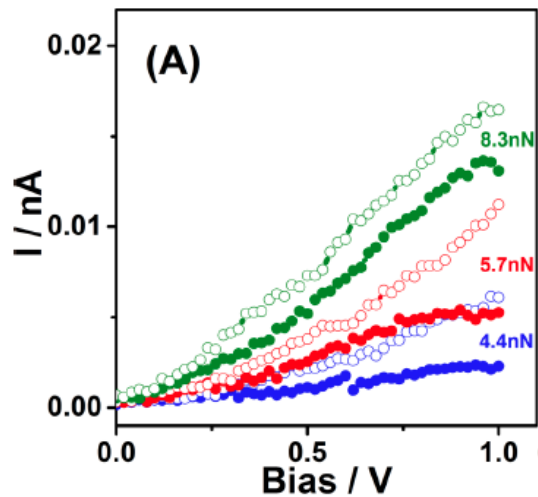
2019

Break junction device built at Yachay Tech
first device of the Quantum Conductance Lab.
Werner Bramer CEPRA Project 2018

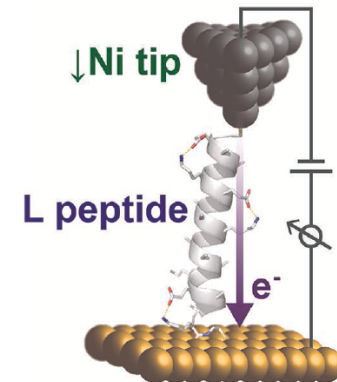
Experiments stretching oligopeptides



monolayers well oriented



Scenario 1



Spin polarization
Is controlled by
strain

Summary of experiments

Usual suspects

- No magnetic fields present
- No magnetic centers (relatively light atoms C, N, O)
- No sources of exchange interactions

Spin polarization intensities

- Polarizations measured larger than those induced by a ferromagnet!
- Chirality a critical ingredient (popular in biol. systems)
- Surfaces appear not to play a role

Where does spin activity come from?

- On the theoretical side we surmised that the spin-orbit interaction was to blame



Change frames
you get a magnetic
field and spin is
oriented

THE JOURNAL OF CHEMICAL PHYSICS **131**, 014707 (2009)

Chiral electron transport: Scattering through helical potentials

Sina Yeganeh,¹ Mark A. Ratner,^{1,a)} Ernesto Medina,² and Vladimiro Mujica^{1,3,b)}

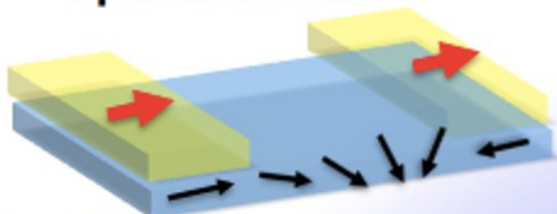
¹Department of Chemistry and Center for Nanofabrication and Molecular Self-Assembly, Northwestern University, Evanston, Illinois 60208-3113, USA

²Laboratorio de Física Estadística de Sistemas Desordenados, Centro de Física, IVIC, Apartado 21827, Caracas 1020A, Venezuela

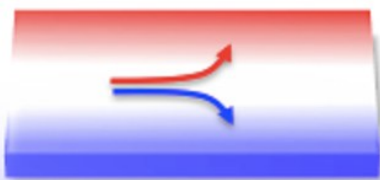
³Argonne National Laboratory, Center for Nanoscale Materials, Argonne, Illinois 60439-4831, USA

(Received 20 March 2009; accepted 10 June 2009; published online 7 July 2009)

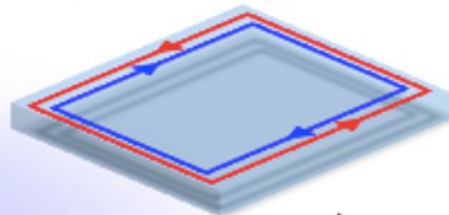
Spin Transistor



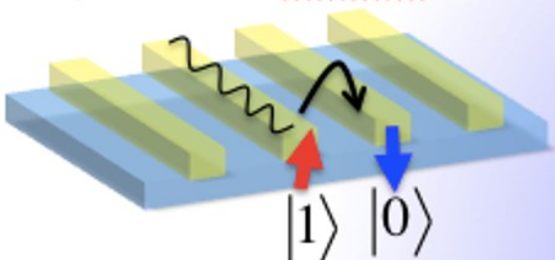
Spin Hall Effect



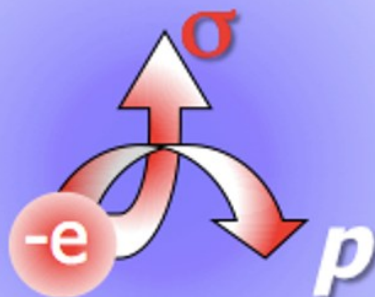
Quantum spin Hall effect



Spin-Orbit Qubits



Spin-Orbit Interaction

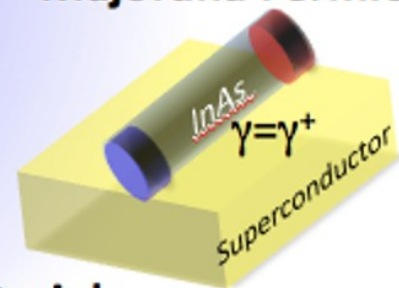


Symmetry breaking

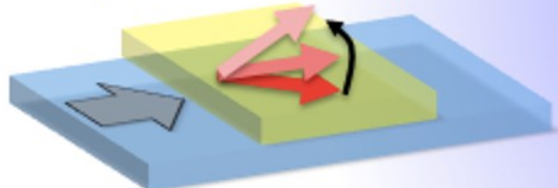
Topological Insulators



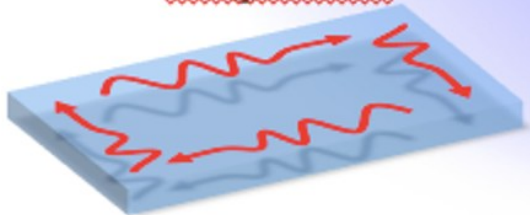
Majorana Fermions



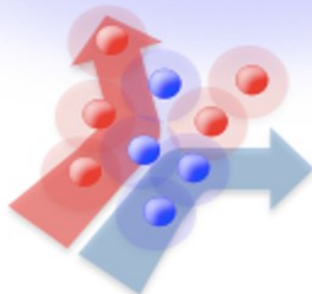
Spin-Orbit Torque



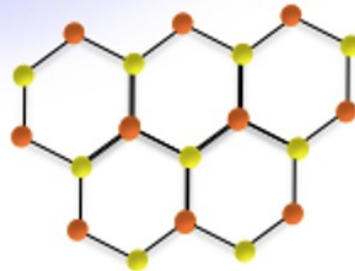
Chiral magnonics



Cold atom systems



Dirac materials



**Spin-orbit everywhere
in recent CMP**

The spin-orbit interaction in the vacuum

- The Spin-orbit interaction in the vacuum (free fields/charges) comes from the Pauli Eq.

$$\mathcal{H} = \frac{p^2}{2m_0} \left[V + V_0 \right] + \frac{e\hbar}{2m_0} \sigma \cdot B - \frac{e\hbar \sigma \cdot p \times \mathcal{E}}{4m_0^2 c^2} - \frac{e\hbar^2}{8m_0^2 c^2} \nabla \cdot \mathcal{E} - \frac{p^4}{8m_0^3 c^2} - \frac{e\hbar p^2}{4m_0^3 c^2} \sigma \cdot B - \frac{(e\hbar B)^2}{8m_0^3 c^2}$$

$$v = 10^6 \text{ m/s}$$

Bare SO interaction

$$\frac{e\hbar \sigma \cdot p \times \mathcal{E}}{4m_0^2 c^2} =$$

$$\mathcal{E} = 10^6 \text{ V/m}$$

$$\mathcal{E} = 10^9 \text{ V/m}$$

$$2 \times 10^{-9} \text{ eV}$$

$$2 \times 10^{-6} \text{ eV}$$

very small bare interaction because of denominator effects

Summary of external sources

- Reasonable external sources of electric field cannot explain the experimental results (eV range) $10^6 - 10^9 \text{ V/m}$
- Electric fields from electronegativity polarization are also too small
- What about internal fields?

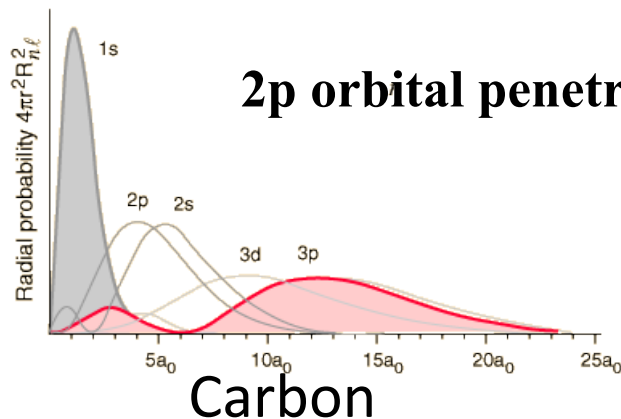
Spin-orbit interaction from atomic source

From the strongest electric fields present: Close to the atomic nucleus

$$\langle p_z | H_{SO} | p_{x,y} \rangle = \langle p_z | \frac{e\hbar}{4m_0^2 c^2} s \cdot (p \times \mathcal{E}) | p_{x,y} \rangle \approx meV \quad \text{Carbon}$$

$$= \frac{(me^4 Z^2 / 2\hbar^2 n^2)^2}{3m_0 c^2}$$

Evaluated at angular momentum of hydrogenic electron exposure to inner cores



Involved fields top 10^{12} V/m

SO from atomic source

- Source of SO is from atomic SO coupling, C, N, O involved (Electric field of atomic cores)

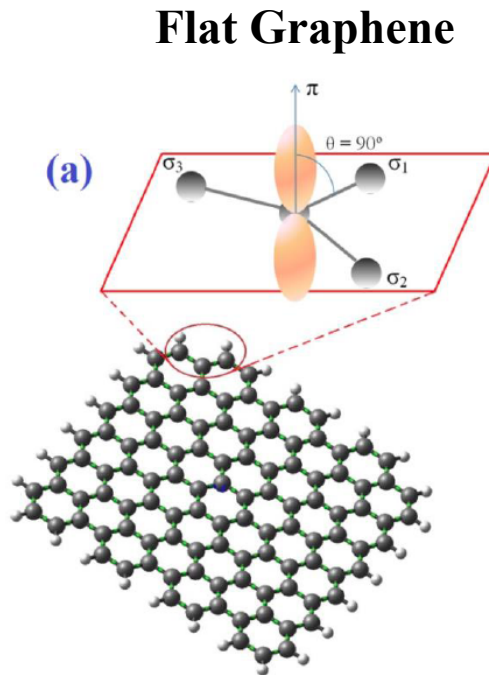
J. Chem. Phys. (2009)
Europhys Lett. (2012)
J. Chem. Phys (2015)
Phys. Rev. B (2016)

Table 3.2. Contribution Δ_j of atom j to the SO splitting Δ_0 from [15]

Be	B	C	N	O	F
0.002	0.004	0.006	0.009	0.010	0.010
Mg	Al	Si	P	S	Cl
0.01	0.024	0.044	0.08	0.09	0.09
Zn	Ga	Ge	As	Se	Br
0.10	0.18	0.29	0.43	0.48	0.49
Cd	In	Sn	Sb	Te	I
0.10	0.36	0.80	1.05	1.10	1.11
Hg	Tl	Pb			
0.5	0.9	2.0			

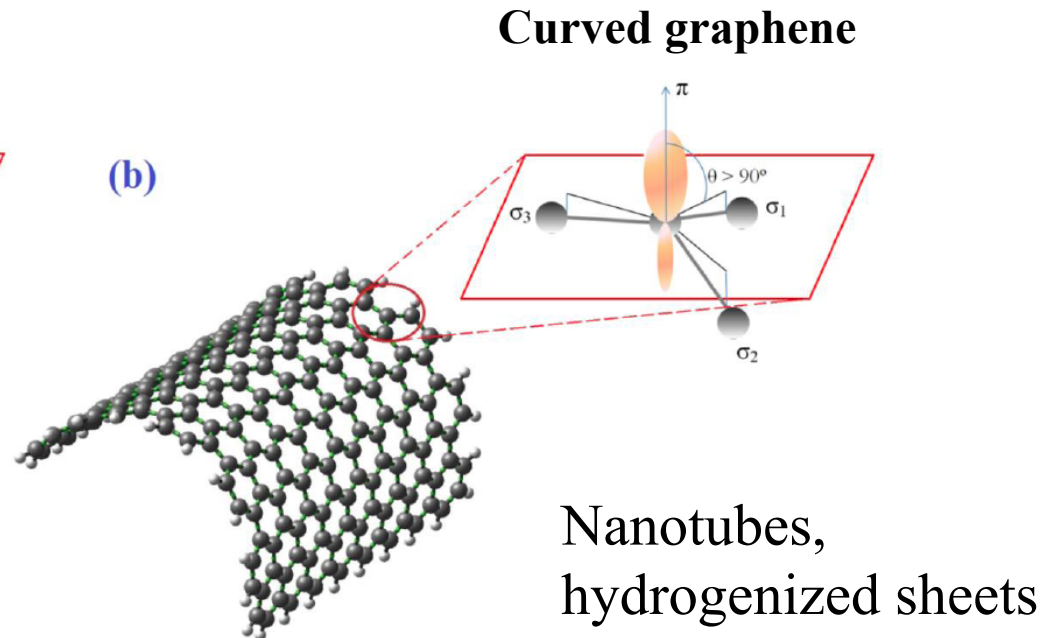
How SO is enhanced by geometry

Example Graphene



SO Coupling = $1\mu eV$

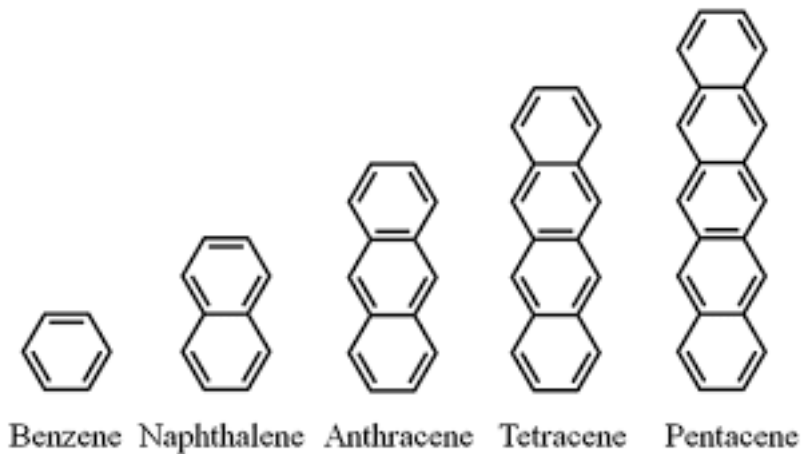
Second order in interaction



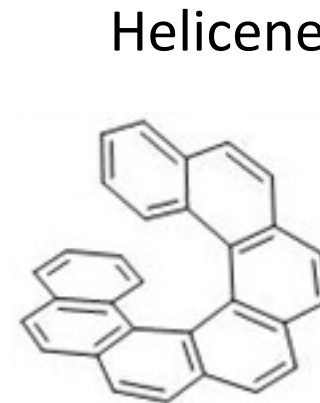
SO Coupling = $1meV$

first order in interaction

Bencene, Naphthalene...versus helicene



Very small SO
second order in
atomic SO

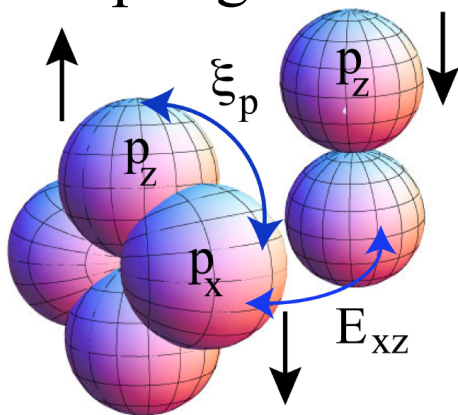


Three orders of magnitude
larger SO, First order in
atomic SO

Evidence SO is coming
from the atomic SO
and the WF overlaps

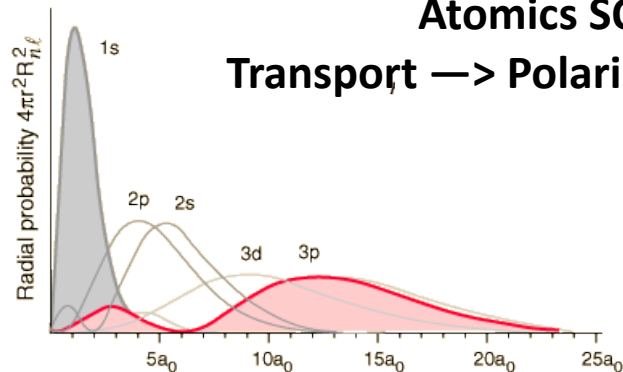
SO from the atomic cores an intuitive approach

SO comes from Atomic coupling



SO Intrinsic

With geometry of DNA



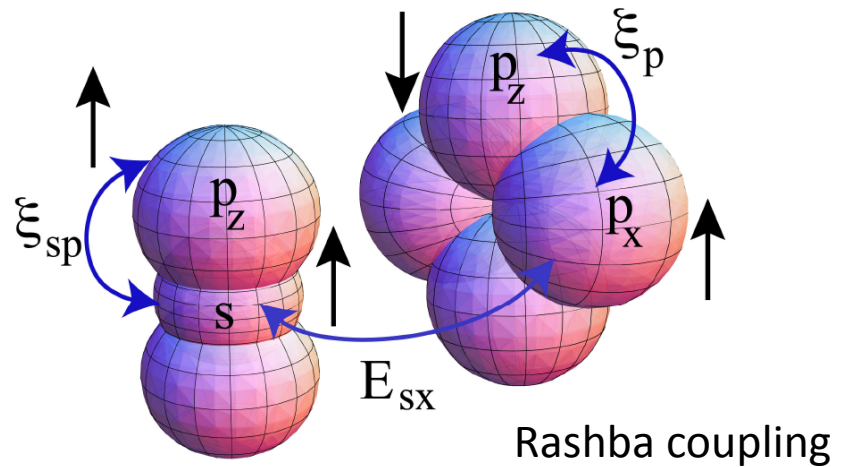
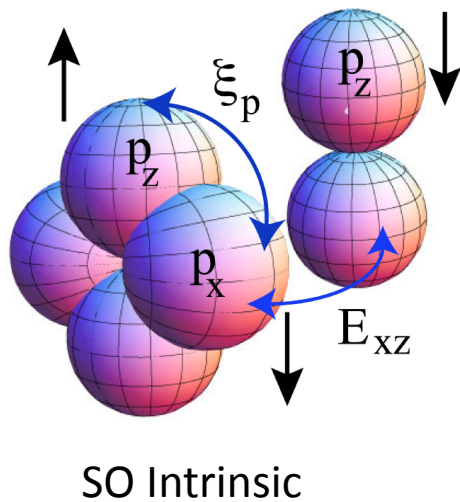
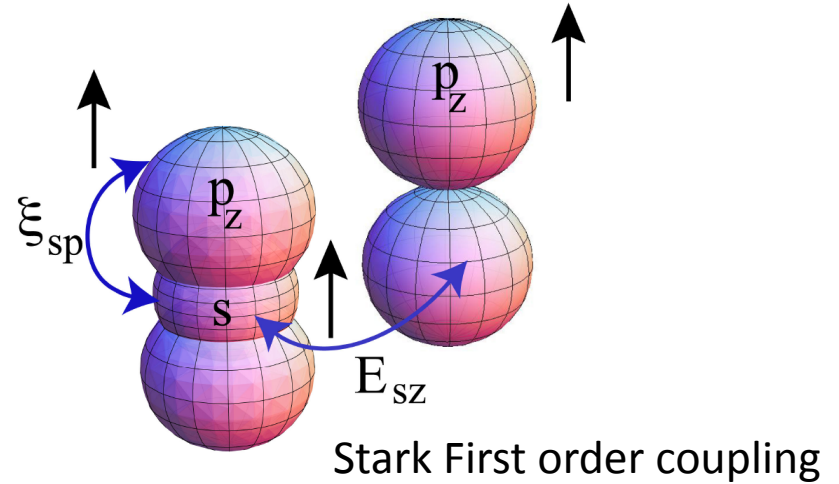
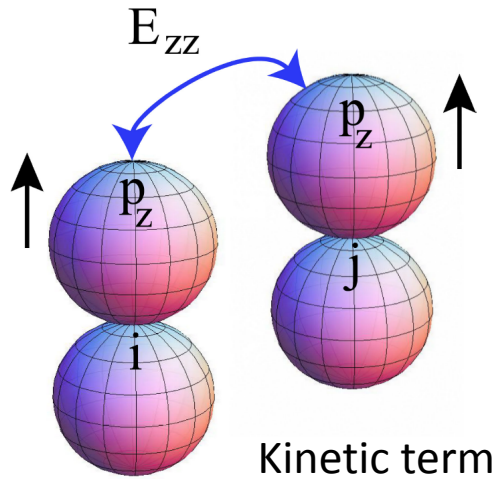
Atomics SO to Transport \rightarrow Polarized electrons

Evaluated at angular momentum of hydrogenic electron exposure to inner cores

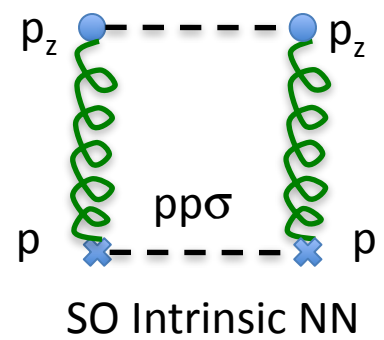
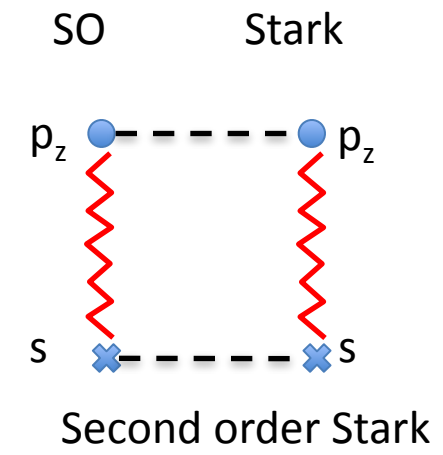
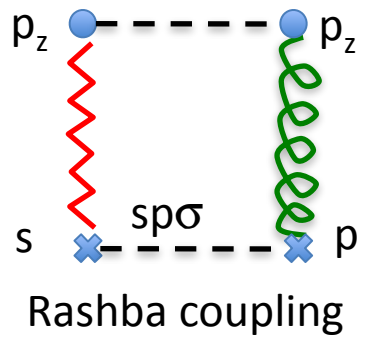
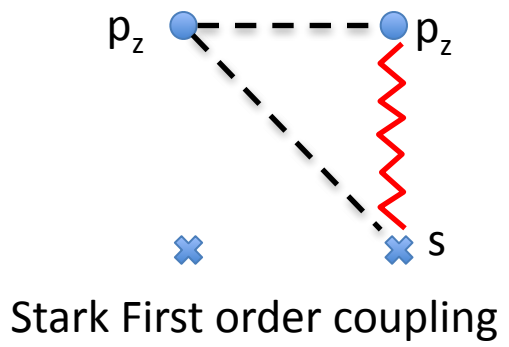
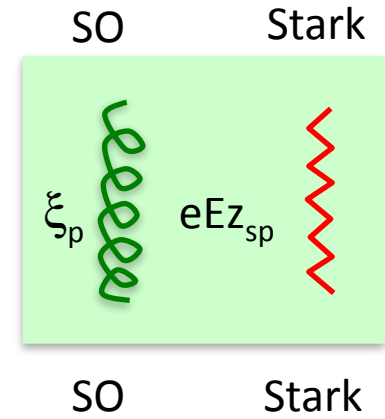
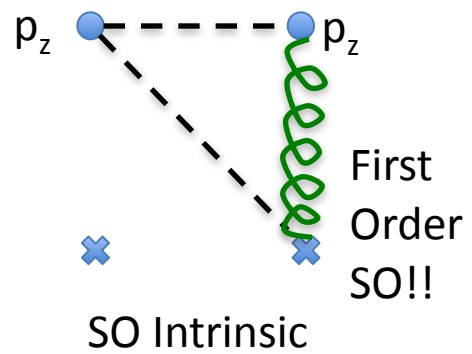
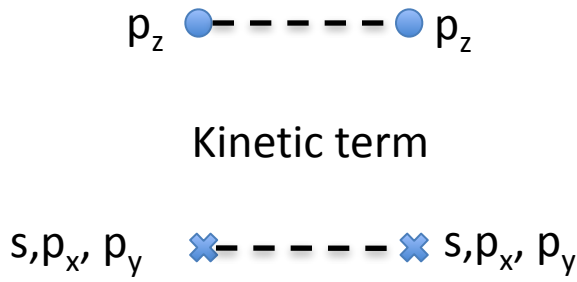
$$\langle p_z | H_{SO} | p_{x,y} \rangle = \langle p_z | \frac{e\hbar}{4m_0^2 c^2} s \cdot (p \times \mathcal{E}) | p_{x,y} \rangle \approx \boxed{meV} \quad \text{Carbon}$$

$$= \frac{(me^4 Z^2 / 2\hbar^2 n^2)^2}{3m_0 c^2} = \xi_p \quad \text{Involved fields top } 10^{12} \text{ V/m}$$

Orbital hoppings

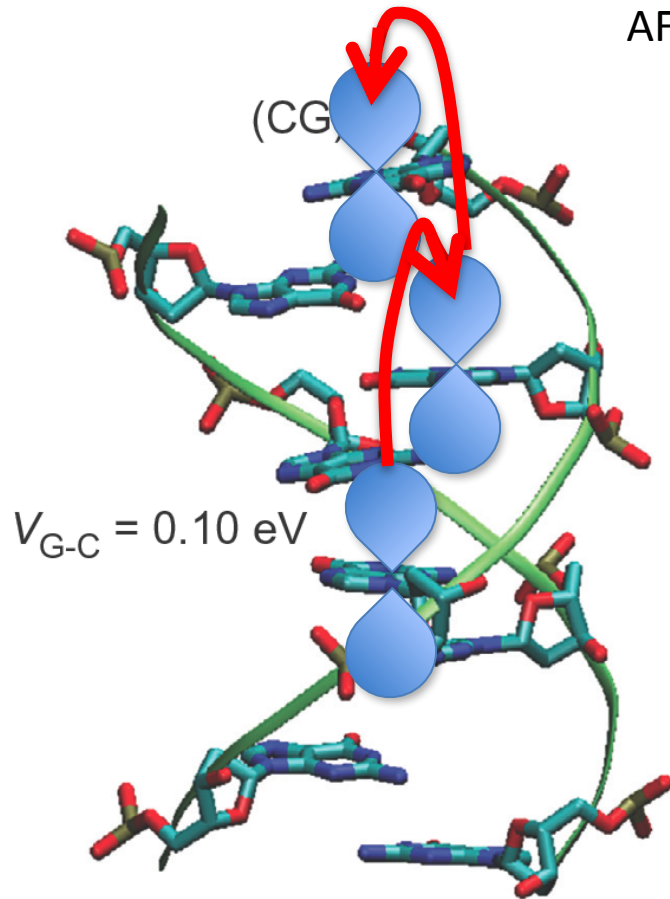


Lowest order terms



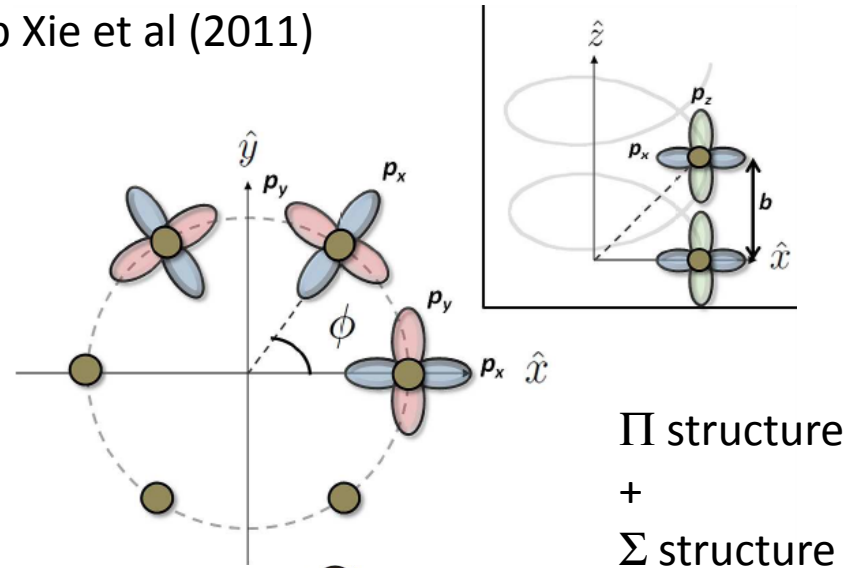
+ NNN terms

Electrons bound to states in molecule



Arrange of orbital results in first order SO coupling

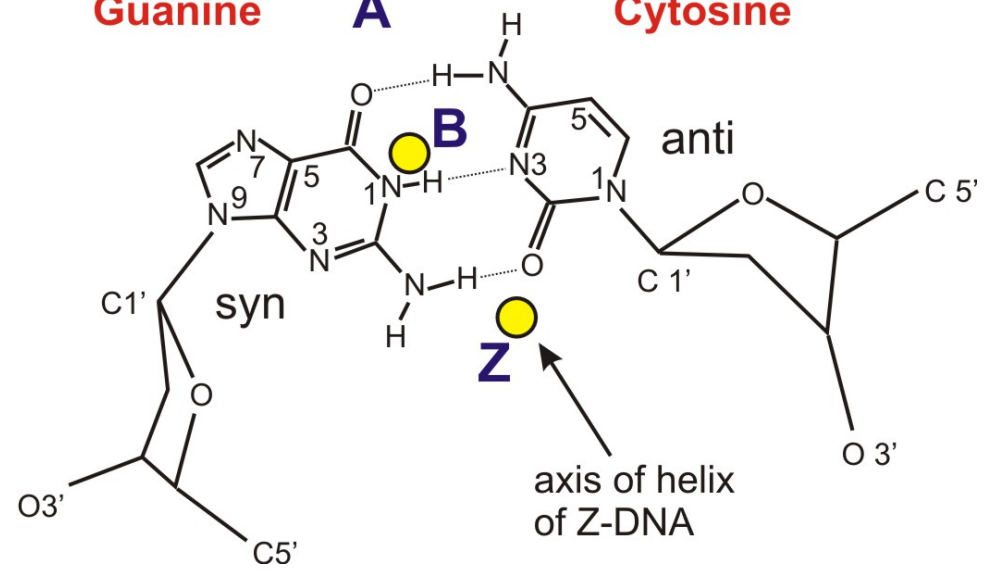
AFM setup Xie et al (2011)



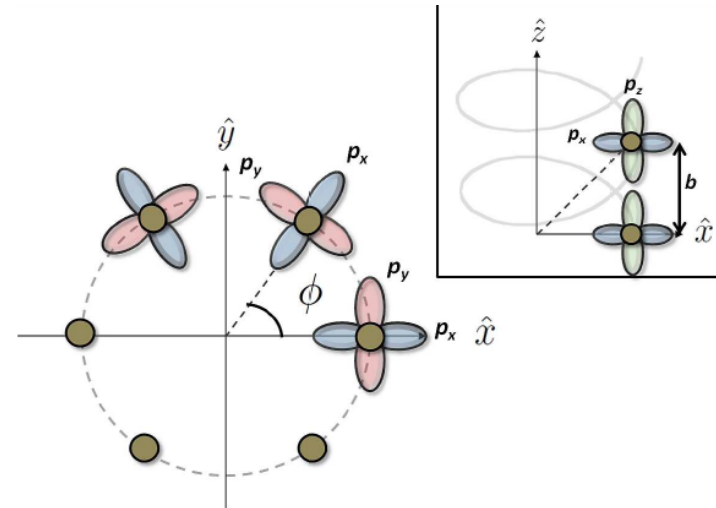
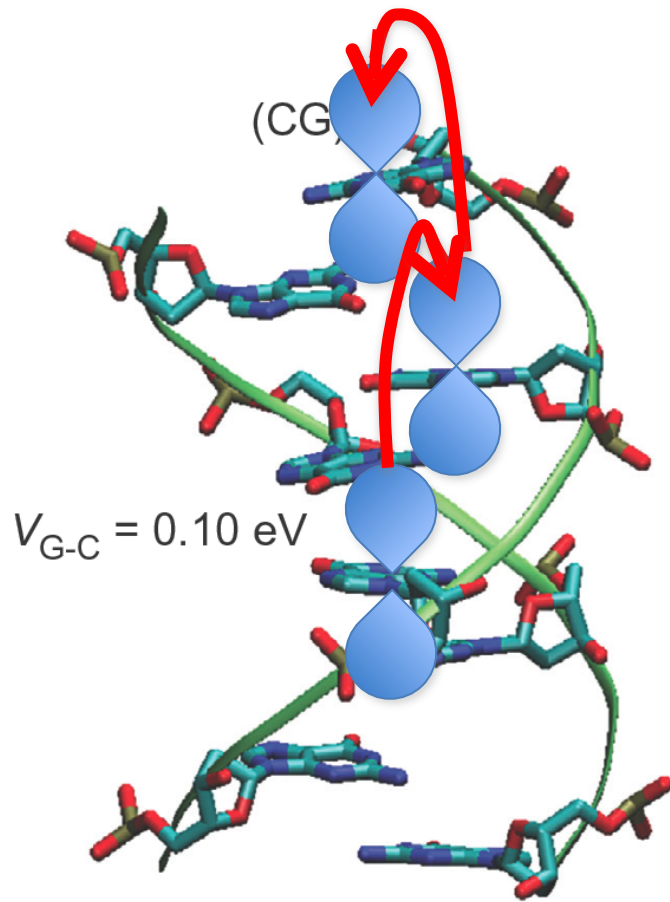
Guanine

A

Cytosine

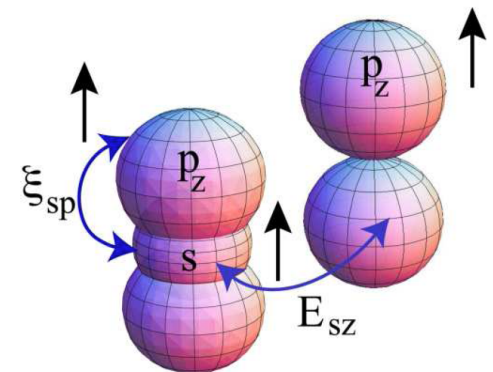
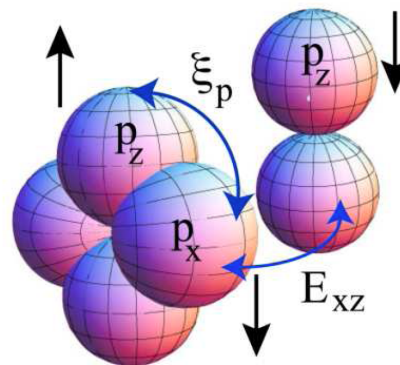


Transport model DNA

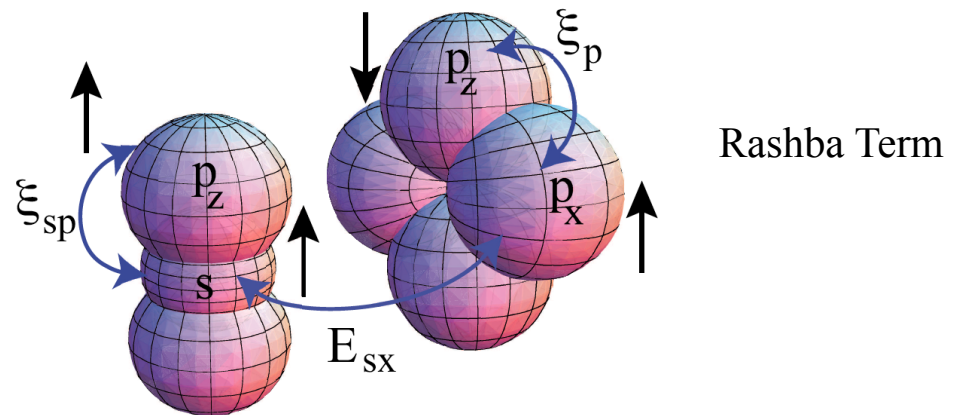
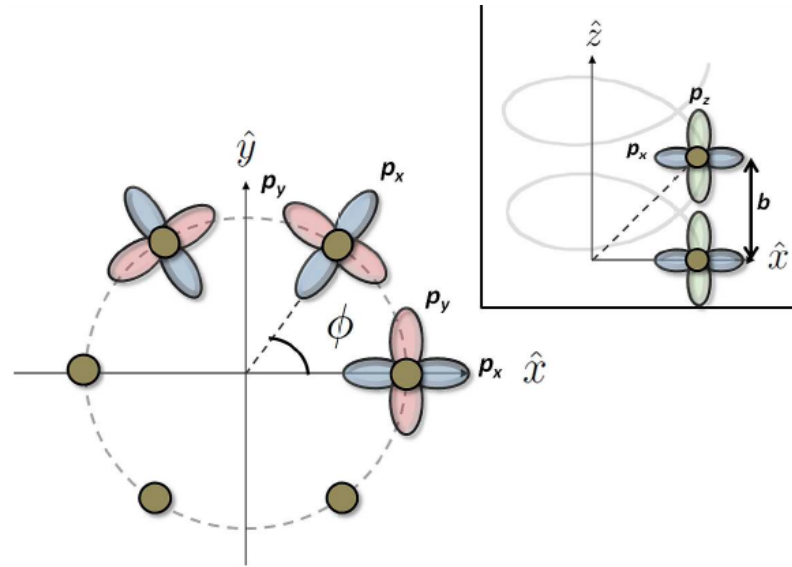
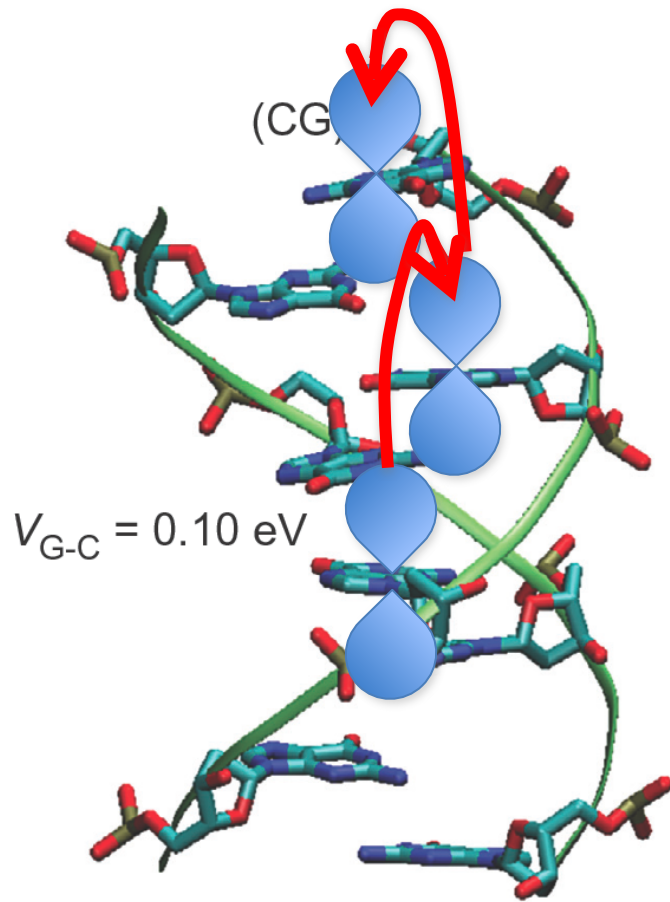


SO 1st order

Stark term 1st order



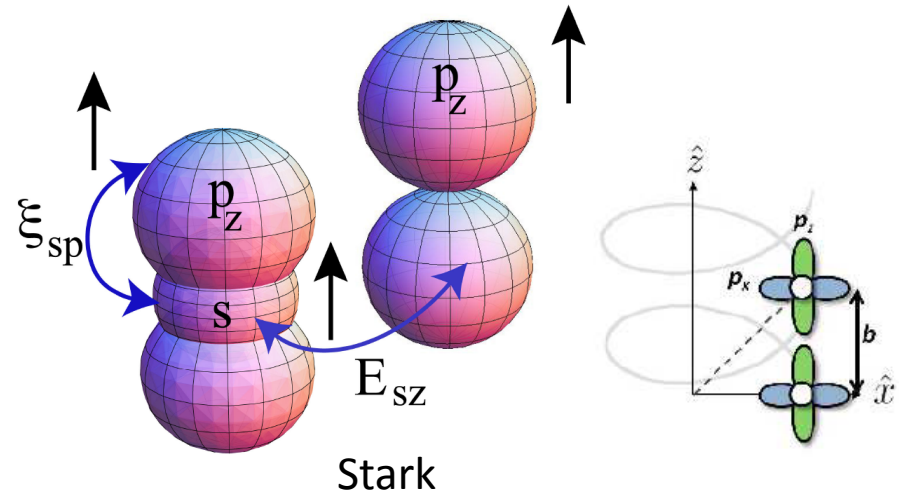
Transport model DNA



Overlaps with DNA twist

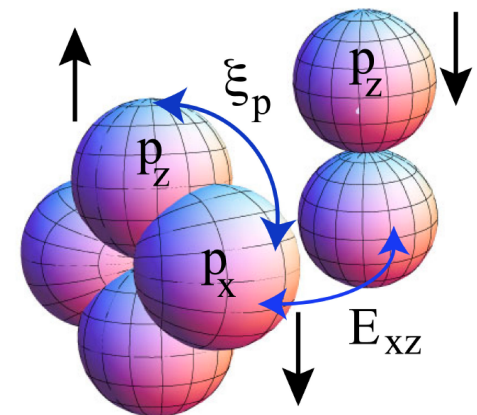
$$E_{sx}^j = \frac{a(1 - \cos \Delta\phi)}{|\mathbf{R}_{j\iota}|} V_{sp}^\sigma = -E_{xs}^j,$$

$$E_{sy}^j = -\frac{a \sin(\phi_j - \phi_\iota)}{|\mathbf{R}_{j\iota}|} V_{sp}^\sigma = -E_{ys}^j$$



$$E_{xz}^j = \frac{2ab \sin^2\left(\frac{\Delta\phi}{2}\right) (\phi_\iota - \phi_j) (V_{pp}^\sigma - V_{pp}^\pi)}{2\pi |\mathbf{R}_{j\iota}|^2} = E_{zx}^j$$

$$E_{yz}^j = \frac{ab \sin(\phi_j - \phi_\iota) (\phi_j - \phi_\iota) (V_{pp}^\sigma - V_{pp}^\pi)}{2\pi |\mathbf{R}_{j\iota}|^2} = E_{zy}^j$$



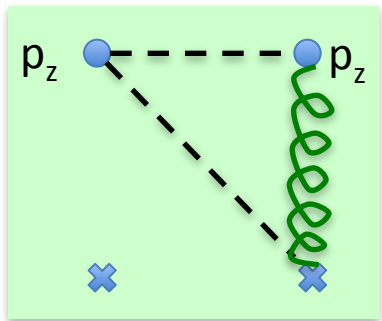
Tight binding Hamiltonian

$$H_K^{in} = \left[V_{pp}^{\pi(in)} + \frac{b^2 \Delta\phi^2 (V_{pp}^{\sigma(in)} - V_{pp}^{\pi(in)})}{8\pi^2 a^2 (1 - \cos \Delta\phi) + b^2 \Delta\phi^2} \right] \sum_{ij} c_i^\dagger c_j,$$

$$= t^{in} \sum_{ij} c_i^\dagger c_j, \quad \text{inside strand (in)}$$

$$H_K^{out} = V_{pp}^{\pi(out)} \sum_{ij} c_i^\dagger c_j,$$

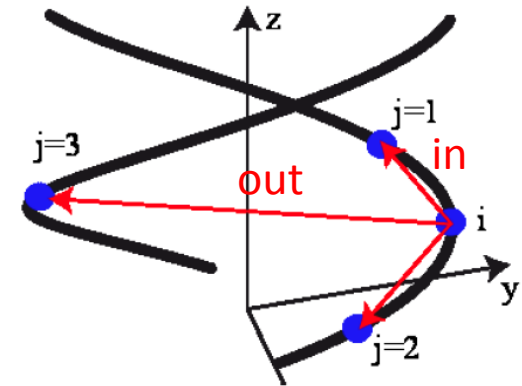
$$= t^{out} \sum_{ij} c_i^\dagger c_j, \quad \text{Between strands (out)}$$



$$H_{SO}^{in} = i\lambda_{SO}^{in} \sum_{ij} c_i^\dagger \nu_{ij} s_y c_j.$$

pitch

SO Intrinsic

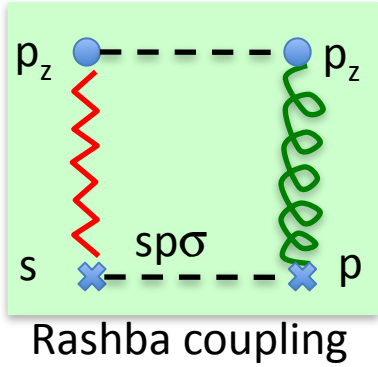


very small
first order SO
between strands

$$\lambda_{SO}^{in} = \frac{4\pi \xi_p ab \Delta\phi (1 - \cos \Delta\phi) (V_{pp}^{\sigma(in)} - V_{pp}^{\pi(in)})}{(\epsilon_{2p}^{\pi} - \epsilon_{2p}^{\sigma}) (8\pi^2 a^2 (1 - \cos \Delta\phi) + b^2 \Delta\phi^2)},$$

Bare SO

Tight binding terms



$$H_R^{in} = i \sum_{ij} c_i^\dagger \left(\lambda_R^{in(1)} s_y + \nu_j \lambda_R^{in(2)} s_x \right) c_j,$$

Rashba Interaction (inside strand)

$$\lambda_R^{in(1)} = \frac{2\pi\xi_p\xi_{sp}a(\cos\Delta\phi - 1)V_{sp}^{in}}{\sqrt{8\pi^2a^2(1 - \cos\Delta\phi) + b^2\Delta\phi^2}} \left[\frac{1}{(\epsilon_{2p}^\pi - \epsilon_{2p}^\sigma)(\epsilon_{2p}^\pi - \epsilon_s) - \frac{2(2\pi a(1 - \cos\Delta\phi)V_{sp}^{in})^2}{8\pi^2a^2(1 - \cos\Delta\phi) + b^2\Delta\phi^2}} - \alpha \right]$$

$$\lambda_R^{in(2)} = -\frac{2\pi\xi_p\xi_{sp}a\sin\Delta\phi V_{sp}^{in}}{\sqrt{8\pi^2a^2(1 - \cos\Delta\phi) + b^2\Delta\phi^2}} \left[\frac{1}{(\epsilon_{2p}^\pi - \epsilon_{2p}^\sigma)(\epsilon_{2p}^\pi - \epsilon_s) - \frac{2(2\pi a\sin\Delta\phi V_{sp}^{in})^2}{8\pi^2a^2(1 - \cos\Delta\phi) + b^2\Delta\phi^2}} + \alpha \right]$$

Tight binding terms

Rashba interaction between strands

$$H_R^{out} = i\lambda_R^{out} \sum_{\langle ij \rangle} c_i^\dagger s_y c_j$$

$$\lambda_R^{out} = \frac{\xi_p \xi_{sp} V_{sp}^{out}}{(\epsilon_{2p}^\pi - \epsilon_s)(\epsilon_{2p}^\pi - \epsilon_{2p}^\sigma) + (V_{sp}^{out})^2}$$

Full lowest order Hamiltonian

$$\begin{aligned} \mathcal{H} = & t^{in} \sum_{\langle ij \rangle}^{helix} c_i^\dagger c_j + t^{out} \sum_{\langle ij \rangle}^{base} c_i^\dagger c_j + i\lambda_{SO}^{in} \sum_{\langle ij \rangle}^{helix} c_i^\dagger \nu_{ij} s_y c_j + i\lambda_R^{in(1)} \sum_{\langle ij \rangle}^{helix} c_i^\dagger s_y c_j \\ & + i\lambda_R^{in(2)} \sum_{\langle ij \rangle}^{helix} c_i^\dagger \nu_{ij} s_x c_j + i\lambda_R^{out} \sum_{\langle ij \rangle}^{base} c_i^\dagger s_y c_j. \end{aligned}$$

Analytical Tight-binding

Effective SO coupling

Bare SO

pitch

$$\lambda_{SO}^{in} = \frac{4\pi\xi_p ab\Delta\phi(1 - \cos \Delta\phi) \left(V_{pp}^{\sigma(in)} - V_{pp}^{\pi(in)} \right)}{(\epsilon_{2p}^{\pi} - \epsilon_{2p}^{\sigma}) (8\pi^2 a^2 (1 - \cos \Delta\phi) + b^2 \Delta\phi^2)}$$

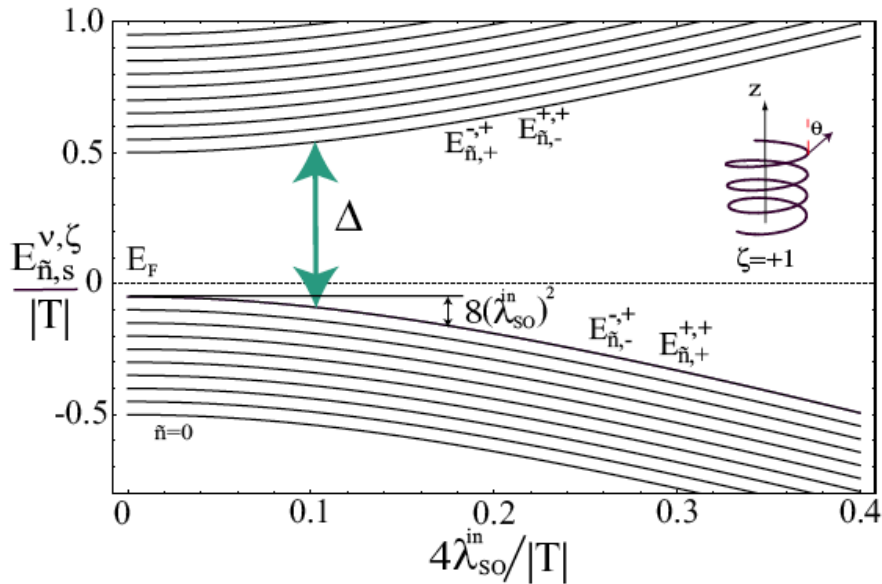
Within each helix

$$\lambda_R^{out} = \frac{\xi_p \xi_{sp} V_{sp}^{out}}{(\epsilon_{2p}^{\pi} - \epsilon_s)(\epsilon_{2p}^{\pi} - \epsilon_{2p}^{\sigma}) + (V_{sp}^{out})^2}$$

Between helices

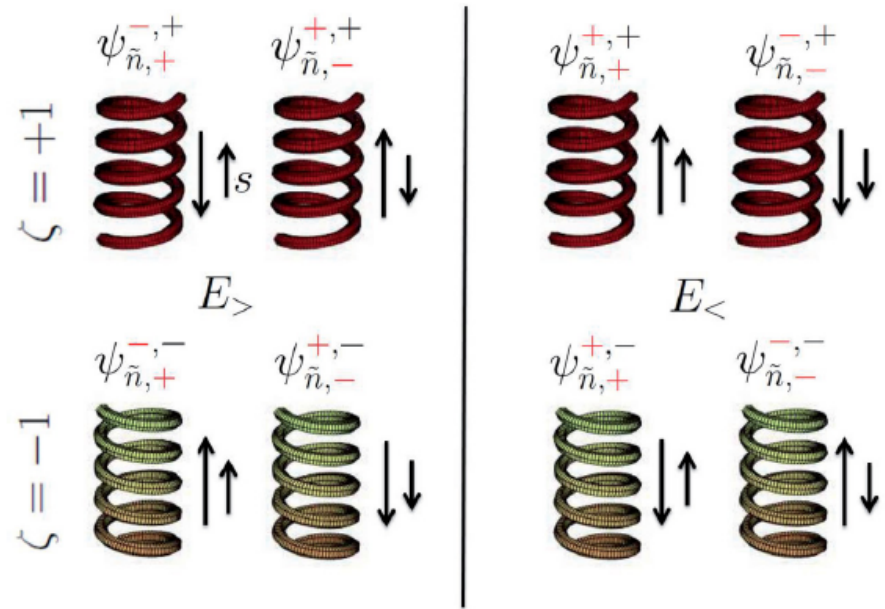
Results

- For DNA specifically (two independent strands)



gap 10 meV < room temp!

Polarization one
order lower than seen in
experiments



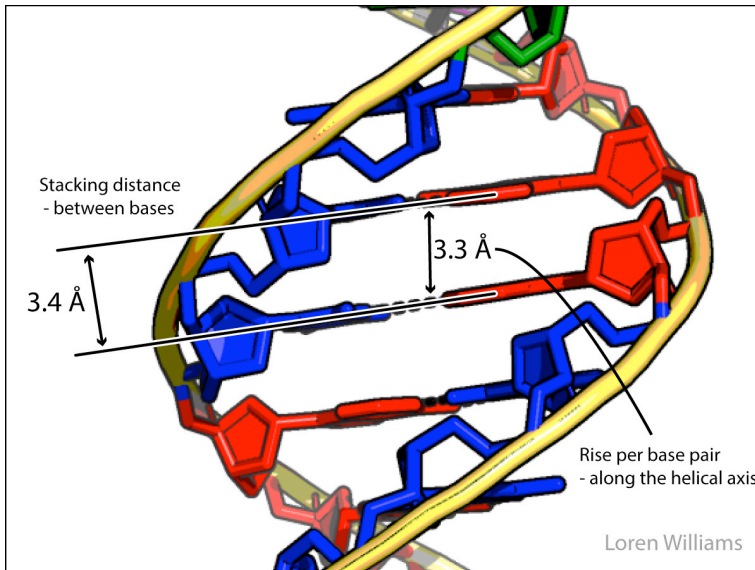
Kramers doublets time reversal
symmetry preserved

As in edge states of Topological insulators

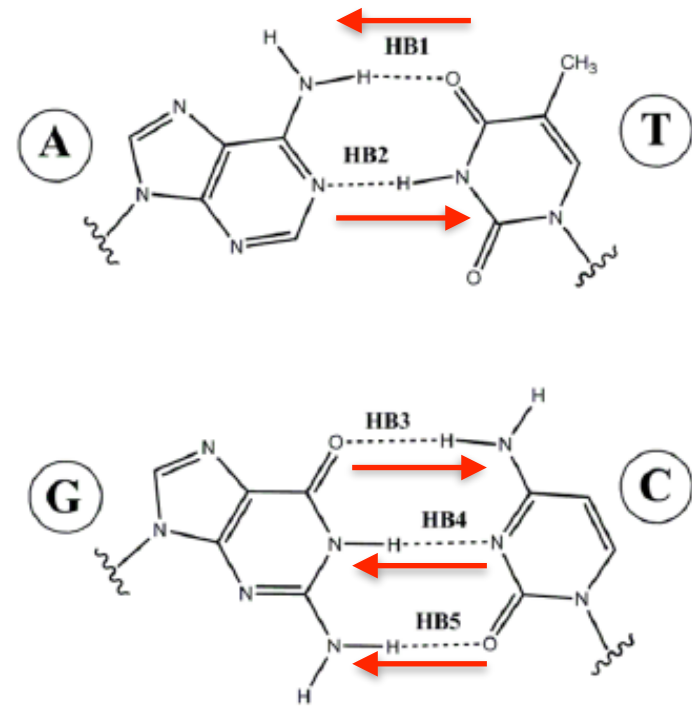
Summary of theory

- Internal source of electric fields
- tight-binding approach gives a broad scenario of the spin effects to be complemented by more detailed calculations
- All qualitative features of the experiment reproduced.... except
 - **MAGNITUDE OF THE EFFECT**

Dipoles in DNA on Hydrogen bonds



Radial Dipoles



Dipoles almost in plane and
tend to cancel out to lower
energy

Hydrogen bonds in oligopeptides

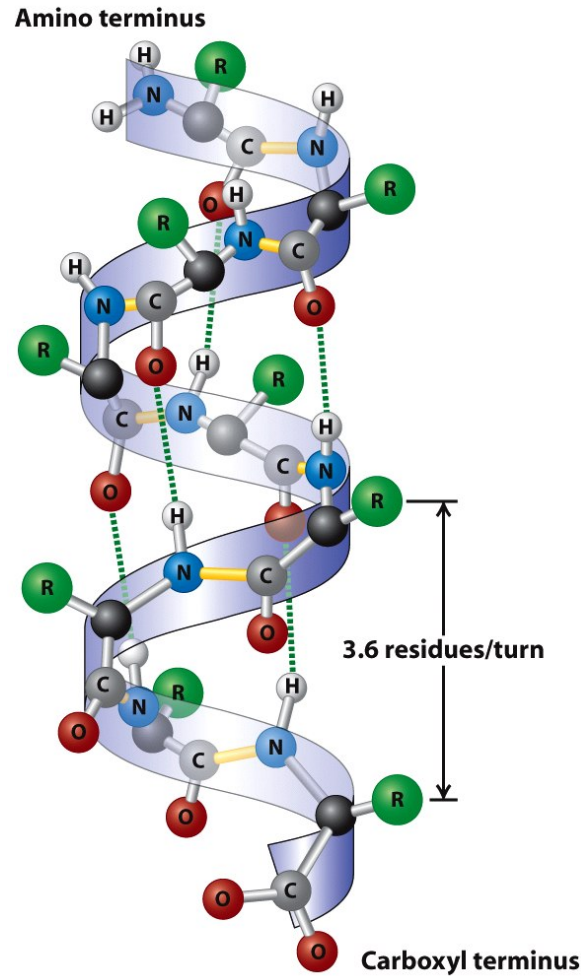
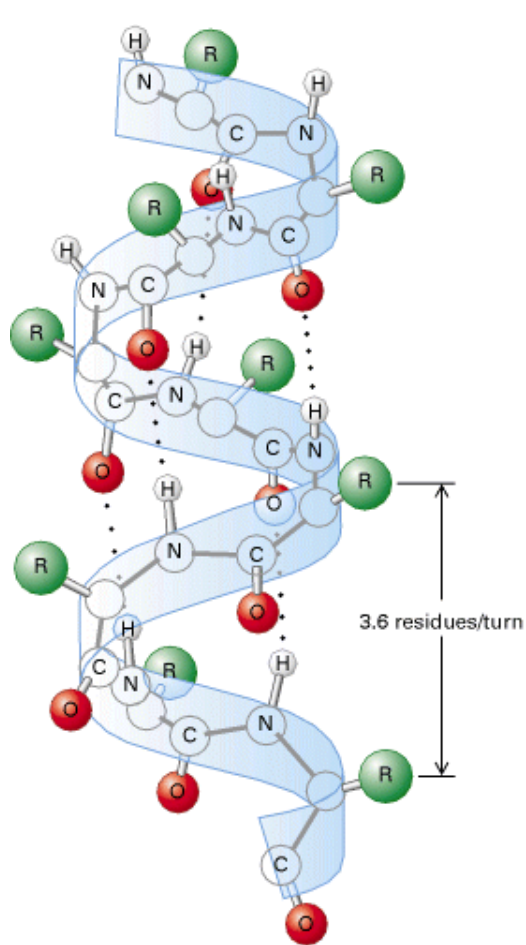


Figure 3-4
Molecular Cell Biology, Sixth Edition
© 2008 W. H. Freeman and Company

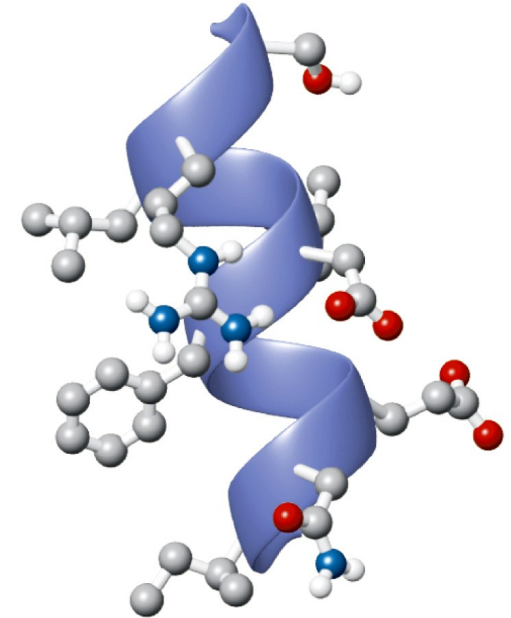
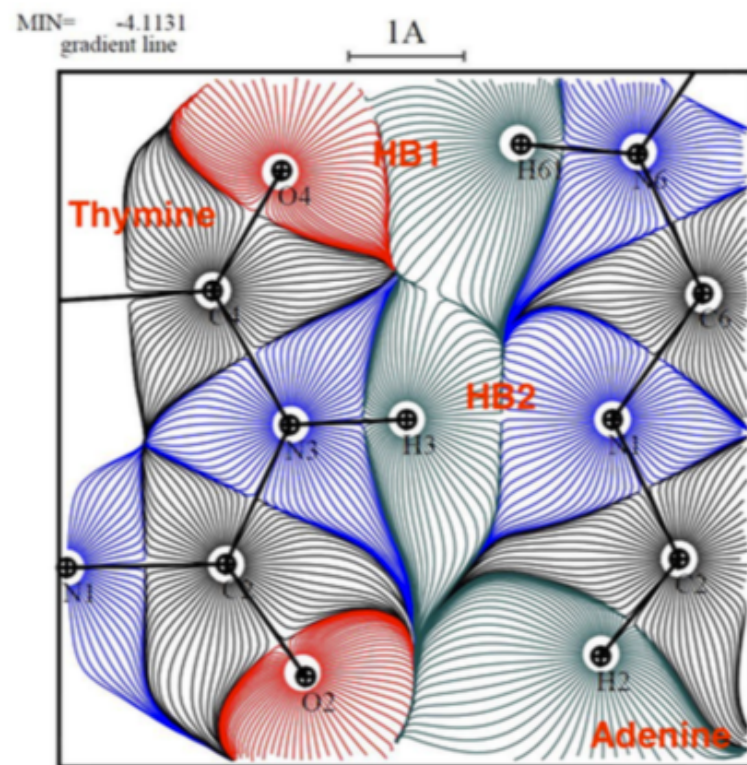
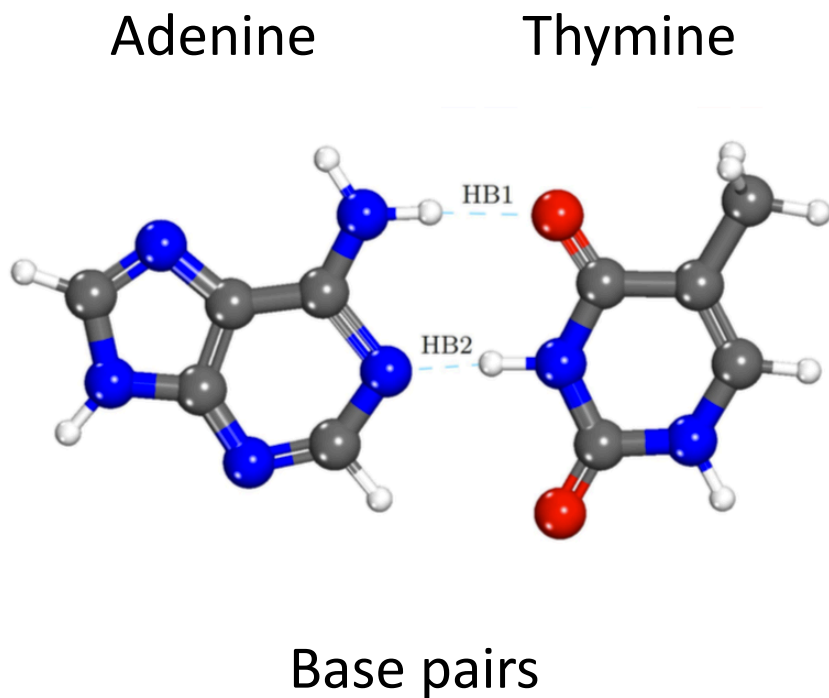


Figure 4-11 Principles of Biochemistry, 4/e
© 2006 Pearson Prentice Hall, Inc.

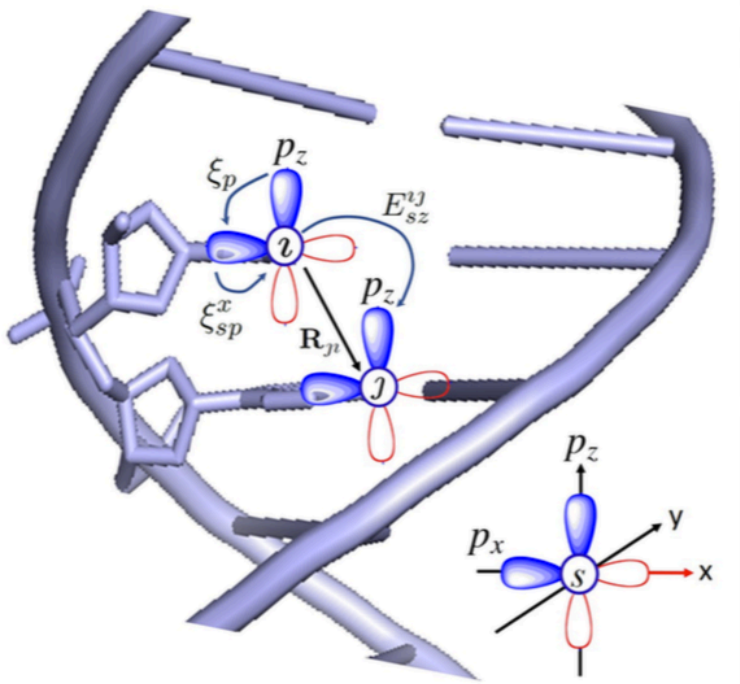
Hidalgo, Torres, Varela
Poster session

Electric fields due to vicinity of hydrogen bonding



Electric field lines and Bader surfaces

Hydrogen bond mediated Rashba

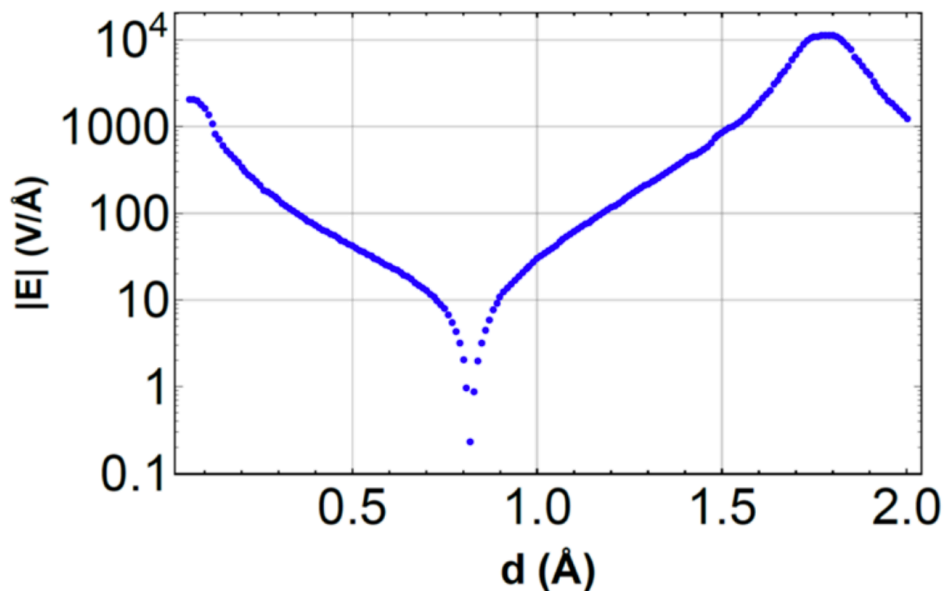


$$H_R = i \sum_{lj} c_l^\dagger (\lambda_R^x s_y + \lambda_R^y s_x + \lambda_R^z s_x) c_j,$$

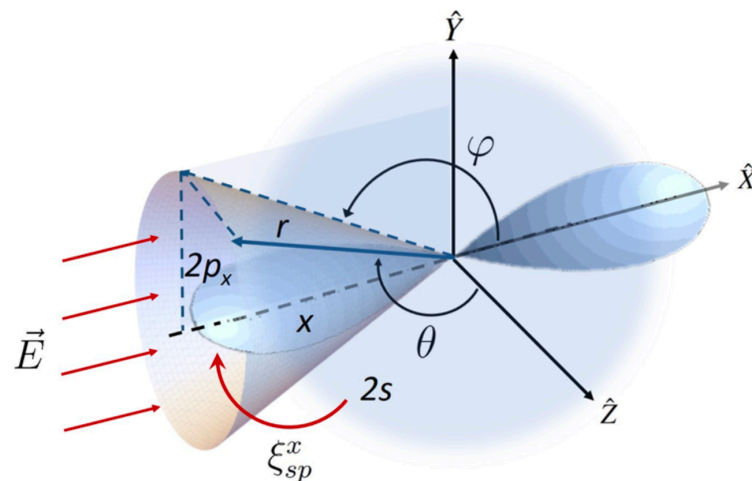
$$\lambda_R^x = - \frac{\xi_p E_{sz}^{lj} [\xi_{sp}^x(l) + \xi_{sp}^x(j)]}{(\epsilon_{2p}^\pi - \epsilon_s)(\epsilon_{2p}^\pi - \epsilon_{2p}^\sigma)},$$

$$\lambda_R^y = \frac{\xi_p E_{sz}^{lj} [\xi_{sp}^y(l) + \xi_{sp}^y(j)]}{(\epsilon_{2p}^\pi - \epsilon_s)(\epsilon_{2p}^\pi - \epsilon_{2p}^\sigma)},$$

Stark interaction with H-Bond electric field



So SO is atomic but Stark is due to the Hydrogen bond another way to increase the effect



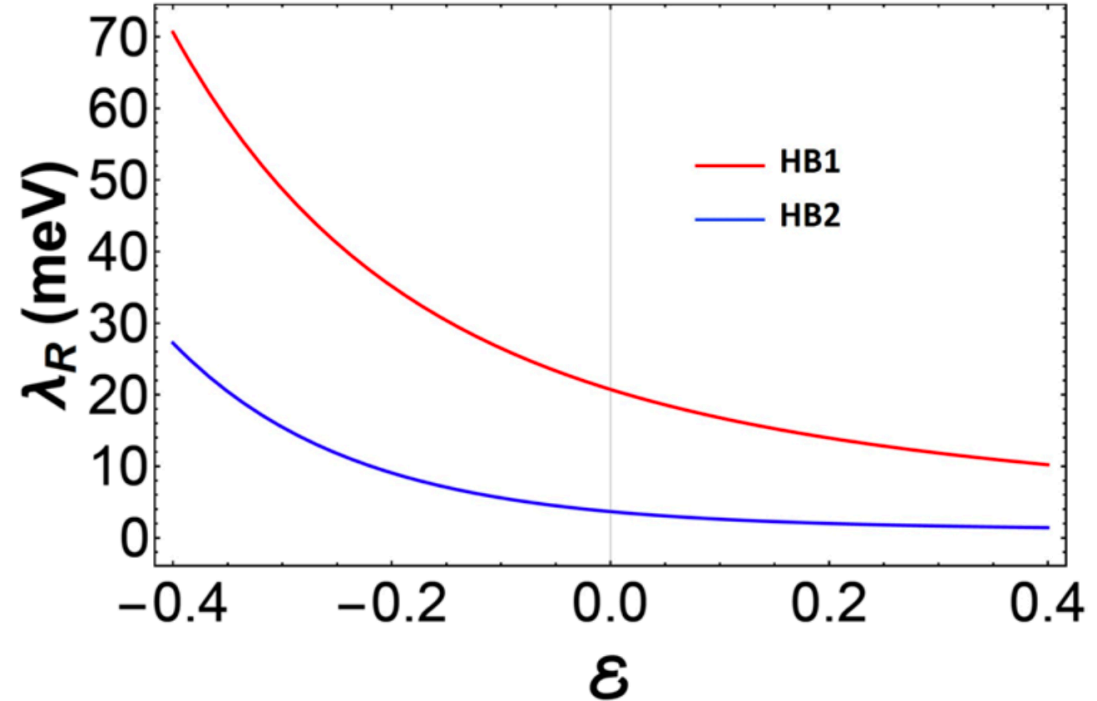
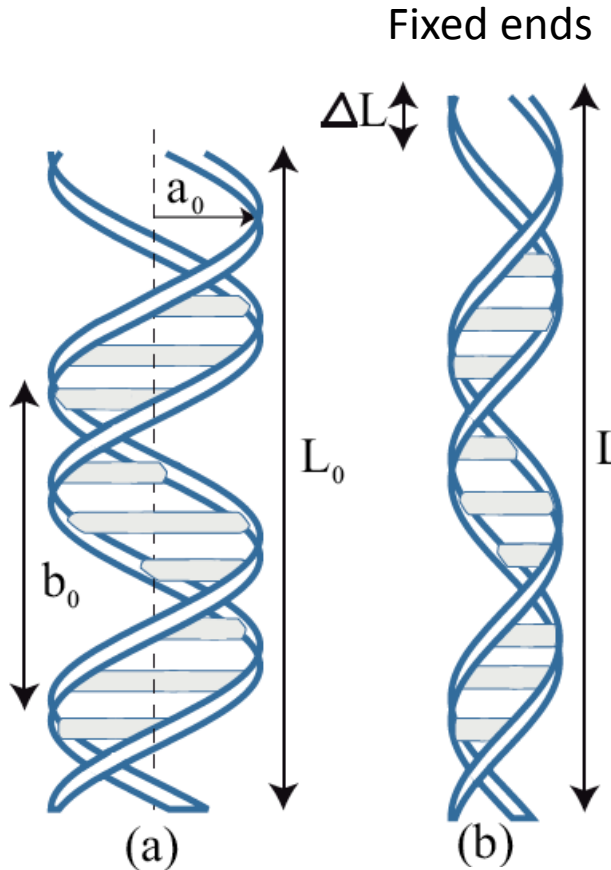
$$\xi_{sp}^i = \langle s | H_s | p_i \rangle = \int_0^{2\pi} \int_0^\pi \int_0^\infty s^* H_s p_i r^2 \sin \theta dr d\theta d\varphi$$

Experimental verification

- How can we prove the previous scenario?
- Perhaps with a new spectroscopy christened:
 - MECHANICAL SPECTROSCOPY

Stretching both ends fixed

Break junction or STM setups

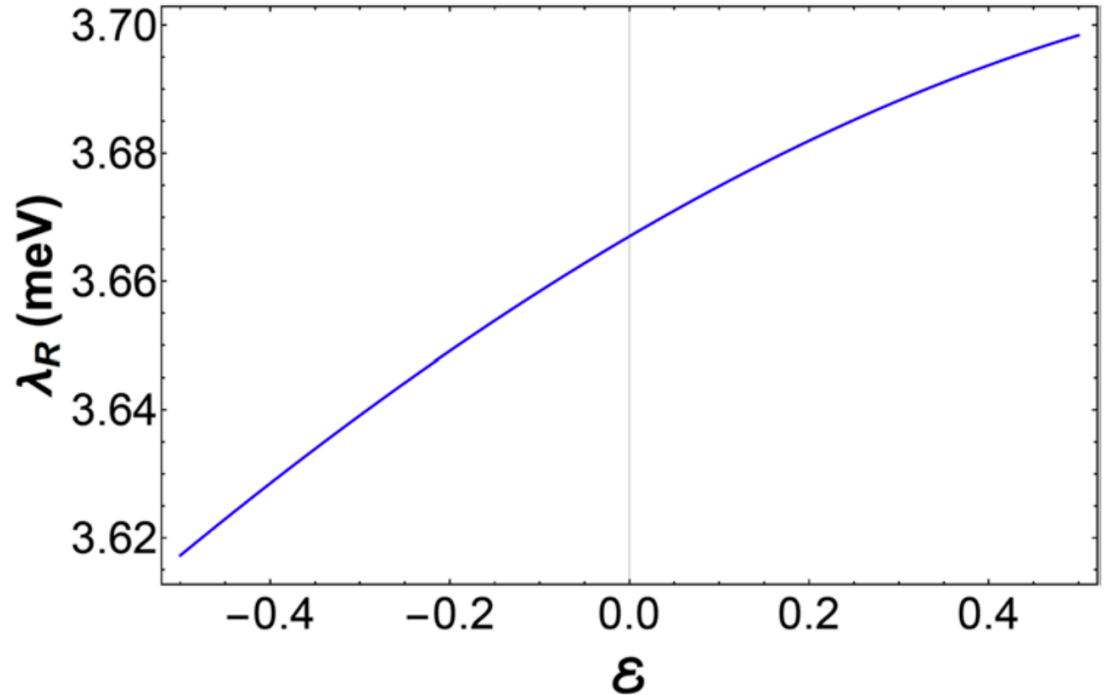
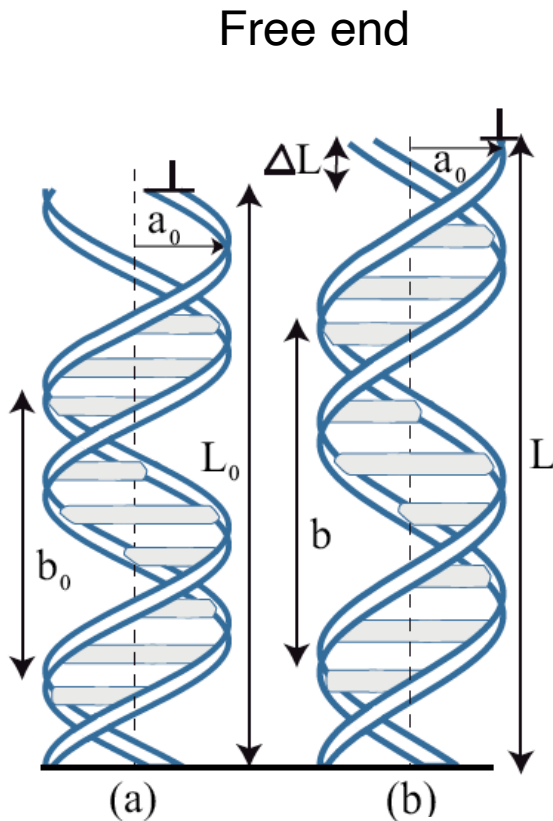


Hydrogen bonds depolarized

Poisson ratio
Reported by
experiments

$$\lambda_R(\epsilon) = \frac{8\pi^2 \hbar^2 \kappa_{ps} \xi_p [\xi_{sp}^{(i)}(\epsilon) + \xi_{sp}^{(j)}(\epsilon)] (b_0 + \frac{L_0}{N} \epsilon) \Delta\phi}{(\epsilon_{2p}^\pi - \epsilon_s)(\epsilon_{2p}^\pi - \epsilon_{2p}^\sigma) m \left[(b_0 + \frac{L_0}{N} \epsilon)^2 \Delta\phi^2 - 8\pi^2 a_0^2 (1 - \nu\epsilon)^2 (\cos\phi - 1) \right]^{3/2}}$$

One free end stretching



Hydrogen bonds untouched

At constant radius a

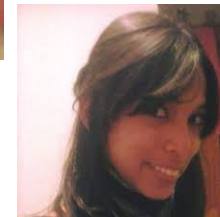
$$V_{\mu\mu'}^{\sigma,\pi} = \kappa_{\mu\mu'}^{\sigma,\pi} \frac{\hbar^2}{m_e R_{2p}^2} \quad \lambda_{SO}(\varepsilon) = \frac{32\pi\hbar^2 \xi_p (\kappa_{pp}^\sigma - \kappa_{pp}^\pi) a_0 L_0 (1 + \varepsilon) \Delta\phi(\varepsilon) \sin^2\left(\frac{\Delta\phi(\varepsilon)}{2}\right)}{m(\epsilon_{2p}^\pi - \epsilon_{2p}^\sigma) \left(16\pi^2 a_0^2 \sin^2\left(\frac{\Delta\phi(\varepsilon)}{2}\right) + b_0^2 (1 + \varepsilon)^2 \Delta\phi(\varepsilon)^2\right)}$$

Conclusions

- Analytical TB approaches coupled to Band folding/ Matrix perturbation/ Renormalization tools can capture major qualitative features of new physical phenomena in low dimensional systems
- Proximity effects (non-bonded interactions/Van der Waals materials) are a novel mechanism to inherit and generate new behavior in low dimensional material.
- TB model can capture interferences between interaction paths that render couplings weak or strong.
- Effects of external fields via the Floquet approach and twisting/warping material next in the pipeline!

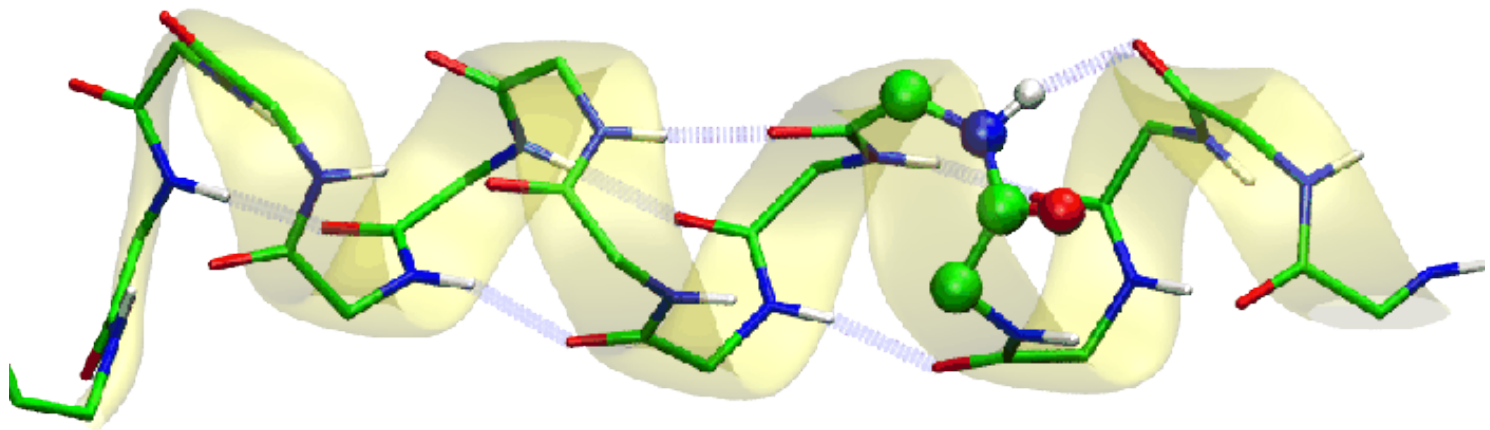
Collaboration

- Solmar Varela, Yachay Tech
- Floralba López, Yachay tech
- Raul Hidalgo
- Juan Torres
- Vladimiro Mujica, ASU
- Bertrand Berche, Lorraine
- Barbara Montañes, IVIC
- Benoit Guillot, Lorraine



Chiral peptide

Made in Nature®



Hidalgo and Torres current patient

Chiral inside chiral